Distribution Agreement

In presenting this thesis as a partial fulfillment of the requirements for a degree from Emory University, I hereby grant to Emory University and its agents the non-exclusive license to archive, make accessible, and display my thesis in whole or in part in all forms of media, now or hereafter now, including display on the World Wide Web. I understand that I may select some access restrictions as part of the online submission of this thesis. I retain all ownership rights to the copyright of the thesis. I also retain the right to use in future works (such as articles or books) all or part of this thesis.

Esther H. Lee April 10, 2016

Investigating the expression of PEZO-1 protein and its involvement with the Emo oocyte phenotype in *C. elegans*

by

Esther H. Lee

Dr. Steven W. L'Hernault
Adviser

Department of Biology

Dr. Steven W. L'Hernault
Adviser

Dr. Guy M. Benian
Committee Member

Dr. William G. Kelly
Committee Member

Dr. Levi Morran
Committee Member
2016

Investigating the expression of PEZO-1 protein and its involvement with the Emo oocyte phenotype in *C. elegans*

By

Esther H. Lee

Dr. Steven W. L'Hernault
Adviser

An abstract of
a thesis submitted to the Faculty of Emory College of Arts and Sciences
of Emory University in partial fulfillment
of the requirements of the degree of
Bachelor of Sciences with Honors

Department of Biology

2016

Abstract

Investigating the expression of PEZO-1 protein and its involvement with the Emo oocyte phenotype in *C. elegans*

By Esther H. Lee

In the nematode *Caenohabiditis elegans*, ovulation is usually tightly coupled to fertilization in the spermatheca after which, like many other animals including humans, meiosis is completed and the zygote begins embryonic development. When defective sperm are present, fertilization in the spermatheca does not occur shortly after ovulation. Such ovulated eggs exit meiosis and begin repeated rounds of mitotic-like replication cycles of their DNA in the absence of cell division, a process named endomitosis (Emo). I investigated the Emo oocyte phenotype and its relationship to the mechanosensory protein PEZO-1 encoded by the C10C5.1 gene in *C. elegans*. Prior work suggested that loss of C10C5.1 function resulted in a nonEmo phenotype, where oocytes would remain paused in meiosis I, even after ovulation and exiting the spermatheca. The C10C5.1 gene is the first gene of the four-gene CEOP4328 operon. I have used million mutation strains, crosses, RT-PCR, and RNAi methods to ensure that only the C10C5.1 gene is involved with the Emo phenotype in *C. elegans*. I have also begun to develop tools that will allow analyses of tissue-specific PEZO-1 expression in the germline and somatic tissues of *C. elegans*.

Investigating the expression of PEZO-1 protein and its involvement with the Emo oocyte phenotype in *C. elegans*

By

Esther H. Lee

Dr. Steven W. L'Hernault
Adviser

A thesis submitted to the Faculty of Emory College of Arts and Sciences
of Emory University in partial fulfillment
of the requirements of the degree of
Bachelor of Sciences with Honors

Department of Biology

2016

Acknowledgements

I would sincerely like to thank Dr. S.W. L'Hernault and his lab in the Biology Department at Emory for all of their guidance and help in growing this past year. Particularly, I would also like to thank Beth Gleason and Huiping Ling who were always willing to help. Thank you to committee members Dr. G. Benian, Dr. W.G. Kelly, and Dr. L. Morran for their patience and guidance throughout this process.

Lastly, thank you to my parents, brother, and friends who supported me throughout this process.

Table of Contents

Chapter 1: Introduction

A) *Caenohabiditis elegans* Reproductive System

The nematode *Caenorhabditus elegans* is found as either a hermaphrodite or a male [1]. Differentiation of gender is determined by X chromosome dosage with two X chromosomes found in hermaphrodites (XX) and one X chromosome found in males (XO) [2-4]. Most of the distinguishable reproductive differences occur during post-embryonic development [3]. The reproductive organs of *C. elegans* develop from somatic gonadal progenitor cells Z1 and Z4 , while the germ line arises from cells Z2 and Z3 postembryonically [5]. In hermaphrodites, the gonadal precursor cells develop into the didelphic (two-armed) symmetrical gonads, while in males they develop into the monodelphic (one-armed) gonad that is asymmetrical [6].

C. elegans hermaphrodites are capable of self-fertilization and hermaphrodites compose the majority of the wild type population, while spontaneous males are only ~0.2% of the wild-type population [7]. Between the two sexes, their reproductive structures differ starkly. The didelphic gonads of the hermaphrodites develop in a symmetric manner from the Z1 and Z4 somatic precursor cells. These cells also give rise to the distal tip cell (DTC), which acts via GLP-1 signaling to regulate the mitotic-to-meiotic transition of the germ line in each gonad [5, 6, 8].

In hermaphrodites, each gonad arm can be divided into three general regions: the distal tip (farthest away from the vulva) to the transition area where the gonad turns 180˚, and the proximal arm where it connects from the looped, U region to the vulva (Figure 1)[6, 9, 10]. The progenitor cells give rise to the distal tip cell that is found in the distal section of each bi-lobed gonad and has been found to regulate the growth and

differentiation of not only the gonad, but also the germ cells, which develops simultaneously [11]. The distal arm of the gonad contains the mitotically-dividing germ cells [12]. The proximal region is the gonadal regions closest to the vulva (at the center of the worm) and it encompasses the oviduct, spermatheca, and uterus (Figure 2). The U-shaped loop in between these two sections is where the germ cells transition from mitotic to meiotic division [9].

As germ cells progress from the distal tip towards the proximal end of each gonadal arm, the germ cells begin to transition and differentiate into sperm or oocytes [9]. Hermaphrodites produce sperm in the L4 stage and begin to produce oocytes after reaching the young adult stage of life and continue doing so throughout its lifespan [13, 14]. The transition from mitotic to meiotic division begins as the germ cells turn from the distal to the proximal region of the gonad. While sperm continue through their meiotic divisions, oocytes develop until they are arrested in diakinesis of meiosis I prophase [15]. In the proximal arm of the gonad, the oocytes continue to develop as they continue down the arm until they are positioned in the oviduct near the spermatheca. The spermatheca is a hollow cavity that holds the sperm and it is where ovulated oocytes are fertilized. The entrance and exit of the spermatheca are smaller than the matured oocytes, so gonadal sheath cells will squeeze the oocytes during ovulation and the walls of the spermatheca dilate to accommodate the volume of the oocyte. The first ovulation will push hermaphrodite-produced spermatids from the proximal arm into the spermatheca where they will become activated into spermatozoa [16]. After fertilization, the embryo exits the spermatheca and moves through the uterus until it is extruded through the vulva [3, 9, 15, 17, 18].

Males are easy to distinguish anatomically from hermaphrodites. Males are smaller than hermaphrodites and have a fan-like tail that is used to help them inseminate hermaphrodites [9, 19]. The gonad of the male is one-armed, however the sperm develop in a similar fashion to that seen in hermaphrodites. In males, the spermatocytes complete meiosis and are stored at the seminal vesicle as spermatids until they are ejaculated [3, 8, 20]. Through unknown mechanisms, the spermatids are activated and undergo spermiogenesis once they are mixed with the seminal fluid during ejaculation [21]. After ejaculation of male-derived sperm into the uterus of the hermaphrodite through the vulva, spermatozoa crawl to the spermatheca where they fertilize oocytes. Male-derived sperm are always able to outcompete hermaphrodite-derived sperm [19, 22, 23].

B) *C. elegans* as model organism and *in vitro* fertilization

C. elegans has been proven to be a great model organism for the study of the reproductive system [1, 24]. Their bodies are transparent, permitting observations *in vivo*, and gametogenesis is relatively fast; spermatocytes to differentiate into spermatids is 90 minutes [25] and oocytes are ovulated every ~20 minutes which is much shorter than other model organisms. In addition, it is easy to create a wide variety of mutant strains with desired defects in specific reproductive genes, including temperature-sensitive mutants [26].

Mutants that affect spermatogenesis are easily identified because they generally fail to lay eggs that are oval and clear with a shell, but instead they lay unfertilized oocytes, which are circular and brown in color [15]. By mating self-sterile hermaphrodites with wild-type males, spermatogenesis mutations can be recovered. Currently more than 60 genes that are associated with spermatogenesis have been

identified and, generally, these mutants are categorized as spermatogenesis-defective (*spe*) or fertilization-defective (*fer*) [24, 27, 28].

Another advantage of *C. elegans* is the ability to isolate sperm in large quantities for use in biochemical assays [29, 30]. There has been extensive work with sperm *in vitro* and the first successful attempt was over 35 years ago by Nelson and Ward in 1980 [16, 27, 31]. Currently the most effective spermatid activator is a serine protease mixture Pronase, however TEA activated *in vitro* sperm have been successfully used to artificially inseminate hermaphrodites [32-34].

All of these techniques have been used to investigate the role of sperm during fertilization. *spe* mutants that are relevant to fertilization are those that have normal morphology and motility but are unable to fertilize oocytes [24, 25, 27, 28]. One of the first candidates to be investigated was the *spe-9* mutant, which is unable to self-fertilize but still produces oocytes that can be fertilized by wild-type males [27]. *spe-9* mutant sperm are motile, have a wild type like appearance in either the light or electron microscope, and can be seen in contact with oocytes. *spe-9* encodes a transmembrane protein that has epidermal growth factor (EGF)-like repeats, which is a protein motif found widely among animal proteins. EGF-like repeats primarily function extracellularly in adhesive and/or ligand-receptor interactions [35]. A number of *spe/fer* mutants are in the "*spe* class" and they include: *spe-9, spe-13, spe-36, spe-38, spe-41, spe-42, spe-45, fer-14* [24, 27].

Despite extensive development of *in vitro* sperm manipulation techniques, there is still no *in vitro* fertilization method available for *C. elegans* research. This is primarily due to the lack of a suitable oocyte donor strain.

When comparing *C. elegans* with humans, there are substantial differences between ovulation in the two species. Although both species produce oocytes that remain paused in meiosis I between diakinesis and metaphase until they are fertilized, if the *C. elegans* oocyte passes unfertilized through the spermatheca, the nucleus exits meiosis, enters mitosis, and undergoes DNA duplication without cell division. This process is called endomitotic replication and is named the Emo phenotype. These unfertilized Emo oocytes transit through the uterus and are inviable if they contact a sperm. Generally, such Emo oocytes exit the vulva and are laid on the growth plate without any signs of fertilization, such as an eggshell [14]. In contrast, human oocytes that are ovulated into the Fallopian tube remain paused in meiosis I and are competent to be fertilized for at least three days [36] [37].

There are also considerable differences between the cell biology of fertilization in *C. elegans* as compared to mammals. Sperm of mammals must penetrate an egg surrounded by cumulus cells and a thick acellular jelly layer named the zona pellucida whereas the sperm of *C. elegans* fertilize an oocyte that lacks any kind of similar surrounding cells or jelly [9, 38]. A mammalian sperm fuses with the oocyte at the equatorial region of the sperm head, while *C. elegans* most likely interact with the oocyte plasma membrane via their pseudopods, which effectively act as their version of flagella [24]. When comparing the reproductive tracts of the two species, the proximal gonad, spermatheca, and uterus of *C. elegans* hermaphrodites can be correlated to the ovary, oviduct (Fallopian tube), and uterus of human females [24, 39].

The mechanisms that allow the sperm and egg to fertilize are not well understood in humans or any other species, despite the availability of *in vitro* fertilization, most

likely due to the lack of suitable mutants. While *C. elegans* has a relatively large collection of sperm mutants that affect fertilization, there has been no oocyte donor strain suitable for *in vitro* fertilization. If *in vitro* fertilization could be achieved in *C. elegans*, interactions between sperm and oocyte in wild type and how they are altered in *spe-9* class mutants could be analyzed.

C) Discovery of the nonEmo phenotype and genetic analysis identifying C10C5.1 as the affected gene

In 1997, McCarter et al. extended the unpublished work of S. L'Hernault and S. Ward on the *him-8(e1462)* mutant strain by showing that unfertilized oocytes remained paused in meiosis after passing through the spermatheca [17, 40, 41]. Due to the lack of endomitotic replication, this is called the nonEmo phenotype. After this discovery, several recombinant strains were created by crossing *fer-1(b232ts)I; dpy-20(e1282)/+ IV* males to *fer-1(b232ts)I; unc-24(e138) him-8(e1462)IV* hermaphrodites [42]. After two generations, individuals with Dpy and Unc progeny were selected and 11 homozygous *fer-1(b232ts)I; unc-24(e138) dpy-20(e1282)IV* recombinants were phenotypically evaluated to see whether they were also homozygous for *him-8* [42]. Sequencing by the Washington University Genome Sequencing Center identified an individual recombinant homozygous for *unc-24(e138) him-8(e1462)* which was then named SL602 [43].

Work by C. Elam and S. W. L'Hernault showed that the nonEmo mutation was located on chromosome IV between *unc-24* and *him-8* (C. Elam and S. W. L'Hernault, unpublished results). Sequencing of the SL602 strain revealed that there were individual mutations in eight separate genes between and including *unc-24* and *him-8.* The well-characterized *unc-24(e138)* and *him-8(e1462)* mutations could be eliminated as causing

the nonEmo phenotype [41, 42]. There was a 18,043 bp deletion, now named *ebDf2*, located from 9,356,671 bp to 9,374,714 bp that removed a sizable portion of the CEOP4328 (located from 9,338,586 bp to 9,366,506-bp), in addition to four other point mutations in nearby genes: C33D9.8, C28D4.5, *gon-1*, and F13B12.6 (Figure 3; [43].

Genetic analyses of the nonEmo region and RNA interference (RNAi) experiments narrowed the candidates to two genes, C33D9.8 and C10C5.1. K. Pohl found that oocytes were nonEmo after passing through the spermatheca in a *fer-1*-containing strain with the C10C5.1(gk208807) opal nonsense stop mutation (from the million mutation project; Thompson, et al. [44]. She also showed that C10C5.1(gk208807) failed to complement *ebDf2* because the *trans* heterozygote showed the nonEmo phenotype, suggesting that loss of C10C5.1 function caused the nonEmo phenotype [43].

E. J. Gleason of the L'Hernault lab confirmed that *C10C5.1/pezo-1* causes the nonEmo phenotype by characterizing multiple strains from the million-mutation project [44], each with a different missense point mutation in the C10C5.1 gene and checking the oocytes for their nuclear phenotype. She found that the C10C5.1 point mutations P1634S, proline to serine, and A2116T, alanine to threonine, were in strains that had a nonEmo oocyte phenotype while the P2235L, proline to leucine, mutation-containing strain produced oocytes that became Emo after passing through the spermatheca (E.J. Gleason, unpublished results). It is possible that certain mutations do not cause loss of function and this seems to be the case for the P2235L mutation.

Further research by the E. J. Gleason has recently discovered that the *pezo-1* gene in *C. elegans* is ubiquitously expressed in both hermaphrodites and males. Reverse transcription polymerase chain reactions (RT-PCR) showed that hermaphrodites from the

feminized strain *fem-1(hc17)*, the masculinized strain *fem-3(q23)*, N2 wild-type hermaphrodites, and *him-8* males all showed expression of the *pezo-1* transcript (Figure 8 and Figure 9). PCRs across the coding region were performed to analyze all of the 12 alternatively spliced mRNA species transcribed from this gene (Figure 3). These strains were chosen because *him-8* males do not produce oocytes and express a male gonad (Figure 1), the *fem-1* and *fem-3* hermaphrodites produce only oocytes or sperm, respectively, while maintaining the same gonad structure typical to N2 wild-type control [45]. After performing RLM-Race, which only amplifies to cDNA those mRNAs that are 5' capped [46, 47], all exons were amplified, except for the segment that started priming from exon 1 of the C10C5.1i and C10C5.1j splice variants. This suggests that many of the *pezo-1* transcripts are ubiquitously expressed in all gonad and germline cells types, although we cannot yet rule out the possibility that there could be differences in the abundance/distribution of one or more isoforms.

C) C10C5.1 and PEZO-1 mechanosensory protein

C10C5.1 is the first gene in the CEOP3428 operon, which also includes three other protein-encoding genes: *T20D3.6, vps-26 (T20D3.7),* and *T20D3.8* [43]. C10C5.1 encodes a mechanosensory protein that is a member of the Piezo protein family. As the *C. elegans* equivalent, it is called PEZO-1 and the longest isoform has 2438 amino acids while the shortest isoform has 1038 amino acids. Few mechanically activated channels are known to date, and the Piezo family of proteins has homologs in many organisms such as mice, *Drosophila melanogaster,* and humans [48]. Although there are two human Piezo proteins, Piezo1 and Piezo2, the protein equivalent in *C. elegans* is called PEZO-1 and correlates with Piezo1 [49]. The secondary structure of Piezo proteins is moderately

conserved and differs from other channel proteins. Generally, Piezo proteins are large transmembrane proteins varying from 2,100 to 4,700 amino acids long with 24-36 transmembrane domains throughout the protein length [48, 49].

Currently, we hypothesize that the PEZO-1 protein is a large transmembrane protein that acts as a cation channel in response to mechanical stimuli, as it has been associated with this response in the mice homolog proteins [49]. In humans, the two Piezo proteins are expressed in the bladder, colon, lungs, and neurons [48]. One reason why this protein family is of such interest is because it is a mechanosensory protein. The underlying mechanisms of many mechanosensory pathways is still unknown [50]. The first discovery of a mechanosensitive protein was in *E. coli* and *Mycobacterium tuberculosis* as proteins MscL and MscS, respectively [51, 52]. Mechanosensory proteins are a heterogeneous group that typically has low expression, and their activity can require the presence of an extracellular matrix and/or cytoskeleton [48].

Although few mechanosensory proteins have been identified in animals, in *C. elegans*, there have been several of these proteins discovered. First, the Chalfie lab discovered a mechanosensitive channel complex composed of the MEC genes associated with sensory neurons [53]. In addition, the transient receptor potential (TRP) protein superfamily has seven subfamilies which all have some members that are associated with mechanosensory functions. Specifically in *C. elegans*, it has been shown that TRP protein can act as an essential pore-forming unit of a mechanosensory channel and that it is playing a direct role in mechanosensation [54, 55].

The Piezo family of proteins has been recently established as another mechanosensory protein that has been most extensively studied in mammals. RNAi

knockdown of gene candidates required for the mechanosensitive currents in mouse N2A cells led to the discovery of *piezo1* gene [49]. In mice, Piezo1 and Piezo2 are expressed in multiple tissues, including bladder, colon, and lung tissues. These proteins contain 24-36 transmembrane segments and are not homologous to any other known ion channels and so have been distinguished as their own family. When overexpressed in mice, the Piezo proteins create mechanosensitive cation currents, suggesting that they act independently of other subunits and probably create a protein pore [48, 56]. Cryo-electron microscopy analysis has shown that mouse Piezo1 has a trimeric propeller-like structure that could use its accessory regions as gates for its ion-conducting pore [57].

Mutations in the human *piezo1* gene have been linked with dehydrated hereditary stomatocytosis as a gain-of-function mutation, familial xerocytosis, and generalized lymphatic dysplasia (GLD), which can be inherited in a dominant autosomal fashion [58-60]. These studies have shown that Piezo1 responds in a domain-like manner signifying that groups of Piezo1 are inactivated or activated together. In addition, patch-clamp electrophysiology research has found that, when it is over-sensitized due to repeated stimulation, Piezo1 has an irreversible loss of inactivation, whereas domain breakage is associated with large or repetitive stimulation [61]. Two models of how Piezo1 could be acting is by being "tethered" to an elastic element so that tension is reduced when the pore is opened or disturbances in the lipid membrane gates the ion pore channel. Recently, some have suggested that the structural data of Piezo1 could point to a mechanism that is intermediary between the two models [62].

Interestingly, Gottlieb et al. [58] noted that the loss of inactivation with repeated stimuli is what had been seen previously in *Xenopus* oocytes, suggesting this cell might

have a channel that is a member of the Piezo transmembrane family [63, 64]. One hypothesized mechanism of mouse Piezo1 inactivation could be due to interactions with the cytoskeleton [65, 66]. In *C. elegans,* the oocytes are continuously pushed along through the gonad from the proximal arm to the vulva. During oocyte meiotic maturation and ovulation, sperm cytoskeletal protein has been linked with signaling to the sheath cells to squeeze the mature oocyte into the spermatheca [67]. Iwasaki et al showed that defects in ovulation led to the Emo phenotype [40]. The mutation of C10C5.1 and its association as a mechanosensory protein implies that mechanosensitive pressures that are associated with oocyte extrusion and development should help us elucidate how these pressures could be influencing the Emo and nonEmo oocyte phenotypes. Our hope is that by determining the cellular location of PEZO-1 protein expression, we would understand how this protein is required to facilitate the Emo phenotype. I hypothesize that PEZO-1 must be expressed in oocytes to facilitate the Emo phenotype.

Chapter 2: Confirming that C10C5.1 is the only gene in CEOP4328 Operon Involved in the nonEmo Phenotype

A) Introduction

The first point mutation in C10C5.1 (*gk208807*) shown to cause the nonEmo phenotype was a premature stop codon. Two other alleles (*gk208807* and *gk364409*) that K. Pohl characterized also had premature stop mutations at other locations in the *pezo-1* transcript. Premature stop codons can trigger nonsense mediated decay that can degrade the entire polycistronic RNA encoded by the an operon via the SMG system in *C. elegans* [68]. The SMG system exists to eliminate mRNAs that encodes premature stop codons and we worried that the polycistronic RNA that encodes *C10C5.1* and its three other

downstream genes might be degraded if there was a nonsense mutation present in C10C5.1. If, in fact, the SMG system was degrading the entire polycistronic RNA transcript, then the other downstream genes could be involved in the nonEmo phenotype. Consequently, all four genes in the CEOP3428 operon had to be evaluated for a possible role in causing the nonEmo phenotype. Previous research in the L'Hernault lab showed that the T20D3.6(*gk208766*) mutant (with a R89C mutation) had Emo oocytes after passing through the spermatheca, so it could be ruled out. This left the *vps-26(T20D3.7)* and *T20D3.8* genes to be evaluated for a possible role in the nonEmo phenotype.

B) Methods

The strains SL1619 and SL1620 which have *fer-1(b232)* on chromosome I and a mutation in T20D3.8(*gk208783;* Y41C) and T20D3.7(*gk773646;* L252P) respectively were created. These specific point mutations were found in strains created as part of the million-mutation project [44] and ordered from the *Caenorhabditis* Genetics Center. Crosses between hermaphrodites that were SL1599 *fer-1(b232ts)*I*; jcIs1 [jam-1::GFP + unc-29(+) + rol-6(su1006)] unc-5(e53)*IV and males that were VC40713(*gk773646*)IV (for the T20D3.7 gene) or VC 30049(*gk208783*)IV (for the T20D3.8 gene) allowed selecting against a GFP marker so that the desired mutation from the million-mutation strains could be put into a *fer-1* background.

Four males were placed with one hermaphrodite per mate plate and, for the F1 generation, nonUnc hermaphrodites were picked to individual plates. These F1 hermaphrodites were allowed to self-fertilize and nonGFP F2 hermaphrodites were picked to their own plates. These nonGFP F2 hermaphrodites should be homozygous for the point mutation on chromosome IV. These nonGFP F2 were allowed to self-fertilize at

16°C and some of their F3 eggs were shifted up to 25°C in order to see whether they were also homozygous for *fer-1,* which causes formation of defective sperm and confers temperature sensitive sterility. Thus, strains that were homozygous for the point mutation on chromosome IV and *fer-1* on chromosome I were obtained.

Hermaphrodites from these strains were grown from birth at 25°C and adults were processed for microscopy. A 5 µL drop of 1X M9 buffer was placed on a positively charged slide, hermaphrodites were picked to the drop, and they were fixed by adding 5 µL of 3% paraformaldehyde/0.1M K_2HPO_4 (pH 7.2) for ten minutes. The slides were washed 2-3 times with 100 µL of PBS-Tween (0.1%). The liquid was removed using a pulled-out Pasteur pipette and 50 µL of ice-cold methanol was added to the slide. The slide was kept at -20°C for 5 minutes and then washed three times with PBS-Tween (0.1%) using a Pasteur pipette. Five µL of Prolong ® Gold Antifade mounting medium with DAPI was added to the slide and a coverslip was placed on top. The slides were left overnight in the dark to dry and the edges of the coverslip were sealed with nail polish the next day. After the nail polish seal dried, the slides were viewed using an Olympus BX60 compound microscope.

C) Results and Discussion

We examined two strains that had a loss of function mutation in either T20D3.7 or T20D3.8, which are two genes downstream from C10C5.1 in the CEOP4328 operon Like the prior investigation of the CEOP3428 downstream gene T20D3.6(*gk208766*) (by Katie Pohl), I found that loss of function T20D3.7 or T20D3.8 mutants had unfertilized oocytes that became Emo after passing through the spermatheca in all self-sterile (due to *fer-1* mutant sperm) hermaphrodites grown at 25°C (Figure 4 and Figure 5). This strongly

indicates that C10C5.1 was the only gene in the four-gene CEOP4328 operon that, when it had a loss of function mutation, was responsible for causing the nonEmo phenotype. Therefore, the nonEmo phenotype initially identified in either of two C10C5.1 opal nonsense stop mutants by Katie Pohl was not due to any secondary effect on the downstream genes of the CEOP4328 operon. In contrast with bacterial operons, the genes within *C. elegans* operons have been found to be less related to one another functionally [69]. My results with the CEOP3428 operon are certainly consistent with this finding about *C. elegans* operons.

Chapter 3: Creation of OD95 *fer-1(b232ts) I*; *ltIs37 IV; ltIs38* strain for visualization of RNA interference (RNAi) caused oocyte phenotypes

A) Introduction

Visualizing the nonEmo phenotype requires that hermaphrodites have sperm that are fertilization-defective so that oocytes that pass through the spermatheca are not fertilized. This is why nonEmo mutants must be crossed into a *fer-1(b232)* background because this mutant confers temperature sensitive sterility at 25˚ due to failure of the spermatozoon membranous organelles (MO) to fuse with the oocyte plasma membrane [24, 25]. Hermaphrodites must be fixed and stained (using the protocol mentioned in Chapter 2) in order to visualize oocyte DNA through a compound microscope. This process makes investigating the nonEmo phenotype time consuming, plus chemical fixation can distort hermaphrodite anatomy. The creation of a strain that uses naturally fluorescent proteins to visualize oocyte chromatin would allow viewing of live *C elegans* during experiments. In addition to anatomy that is undistorted by fixation, live worms

would also allow dynamic visualization of oocytes as they matured and aged in the uterus.

In order to study the gonad and early embryo of *C. elegans*, several methods have been developed that permit fluorescent protein expression and visualization in the germline using ballistic bombardment, mating, and various other live imaging techniques. OD95 *unc-119(ed3) III; ltIs37 IV; ltIs38* is a line created by ballistic bombardment with insertions *ltIs37* [(pAA64) *pie-1p::mCherry::his-58 + unc-119(+)*] and *ltIs38* [pAA1; *pie-1::GFP::*PH(PLC1delta1) + *unc-119(+)*], respectively conferring red staining of histones in oocyte chromatin and green staining of the oocyte plasma membrane [70]

B) Methods

Four *fer-1(b232ts)*I males were crossed with one hermaphrodite from the OD95 *unc-119(ed3)*III*; ltIs37*IV*; ltIs38* line. One F1 was placed on an individual plate and was allowed to self-fertilize. From the F2 generation, hermaphrodites that were bright red and had a nonUnc phenotype were picked to their own plates. After allowing self-fertilization, some of the F3 eggs were shifted to 25°C to look for sterility and confirm that those individuals were homozygous for *fer-1* on chromosome I. This strain could be visualized in the compound microscope after methanol fixation and DAPI staining, or live worms could be paralyzed by putting them on a positively charged slide and adding 4-8 μL of 1mM levamisole.

C) Results

OD95 *fer-1(b232ts)*I; *ltIs37*IV*; ltIs38* showed bright red chromatin in the dissecting (not shown) and compound microscopes, however the distinction between nonEmo oocytes, Emo oocytes, and eggs were only observable in the compound

microscope (Figure 6 and 7). In addition, the green fluorescence around the oocytes membranes was too dim to be visualized in the dissecting scope or at low magnification in the compound microscope.

D) Discussion

The OD95 *fer-1(b232ts)*I; *ltIs37*IV*; ltIs38* strain can be used to visualize the nonEmo phenotype in oocytes of *C. elegans* without fixation and staining. This will be especially useful for RNAi experiments and should confirm the already-obtained DAPI staining results. Because *pezo-1* is located on chromosome IV, where the OD95 mCherry inserted *ltIs37* transgene that marks chromatin is also located, genetic recombination is needed to create the double mutant.

Recently, E. J. Gleason of the L'Hernault lab has successfully crossed OD95 *fer-1(b232ts)*I; *ltIs37*IV*; ltIs3* males with SL1573 *fer-1(b232ts)*I*; unc- 24(e138) dpy-20(e1282)*IV hermaphrodites (this strain bears the 18,043 bp deletion that removes *pezo-1*). So far, we can tell that the mCherry insert is located on chromosome IV closer to *unc-24* than it is to *dpy-20* because all of the Unc nonDpy recombinants do not have mCherry-associated red fluorescence whereas 5 of the 12 Dpy nonUnc recombinants show red chromatin fluorescence in the dissecting microscope. After shifting F3 eggs from potential recombinants to 25°C, they were viewed in the compound microscope to see if the *pezo-1* deletion mutation recombined onto the *ltIs37*-bearing chromosome. E. J. Gleason found that the *pezo-1* deletion mutation was picked up by a few of the Dpy nonUnc recombinants (unpublished results).

The creation of OD95 strains with the *pezo-1* mutation +/- the temperature sensitive *fer-1* mutation will facilitate future investigations into how the PEZO-1 protein

causes the Emo oocyte phenotype. Particularly, it has been helpful in looking at the results of RNAi experiments, as will be shown in the next chapter.

Chapter 4: RNAi methods

A) Introduction

Some genes lack available mutations and RNAi has been developed as an alternative approach to generating a loss of function phenotype for any gene in many organisms, including *C. elegans* [71, 72]. After Fire and Mello published their results on injecting double stranded RNA (dsRNA) into nematodes in 1998, alternative methods of bacterial feeding, liquid feeding, and soaking were also developed, including the creation of RNAi libraries [73]. Once the dsRNA is in the body of the worm, a large protein complex called Dicer complex will process the dsRNA into short interfering RNAs (siRNAs) that can now guide the RNA induced silencing complex (RISC) to cleave mRNA targets. RNAi in *C. elegans* can be inherited as the progeny of the injected worms sometimes show a knockdown phenotype [74]. In addition, systemic RNAi is has been shown to require the transmembrane protein SID-1, which allows the spreading of RNAi silencing to cells away from the initial source tissue of dsRNA [73, 75].

B) Use of *eri-1* and *rrf-3* to differentially enhance RNAi

Loss of function mutations in *C. elegans* genes involved in the RNAi process produce worms that show differentially higher RNAi sensitivity in certain tissues. One of the first such strains to be discovered was the *rrf-3* mutant, which affects a RNA dependent RNA polymerase (RdRP) that regulates the accumulation of siRNAs [74]. Several studies have confirmed that mutations in the *rrf-3* gene confer enhanced RNAi sensitivity when compared to wild type [76, 77]. Another gene, *eri-1,* encodes an

exonuclease that acts as a negative regulator of RNAi. Mutations in this gene caused an enhanced RNA interference (Eri) phenotype, and this strain also shows enhanced RNAi sensitivity in tissues where *rrf-3* has not been useful [78, 79]. In a study comparing tissue specificity to RNAi methods [80], the *rrf-3* strain was found to be more sensitive than *eri-1* in the gonad and both were more sensitive in the gonad and germline when compared to wild type N2 strain. This differential sensitivity in the somatic gonad and germline could possibly tell us whether *pezo-1* expression prevents the nonEmo phenotype through its specific action in only one of these two tissues.

B.1) Methods

We fed bacteria expressing double stranded RNAs to four different *C. elegans* strains: *rrf-3, eri-1, fer-1,* and OD95 *fer-1(b232ts)*I; *unc-119(ed3)*III*; ltIs37*IV*; ltIs3.* All the worm strains were temperature sensitive sterile. Five different RNAi vectors were fed to the worms, four of which came from the Ahringer RNAi library, which has genomic DNA inserts in the L4440 vector [81, 82]. The negative control was an L4440 vector that did not have a recombinant insert and the positive control was the L4440 vector containing a *gon-1* insert; loss of function *gon-1* mutants show a very distinctive loss of gonad phenotype [83]. The experimental RNAi strains taken from the Ahringer library targeted C10C5.1(exons 1-6) and C10C5.1(exons19/20-21/22). The latter was initially recorded as gene T20D3.11 because it was thought to have been a separate protein, but was later discovered to be part of the *pezo-1* gene. The third experimental trial was created by inserting a portion of the *pezo-1* cDNA transcript (obtained by RT-PCR using inserts EL23/24) into the L4440 vector as a 165 bp insert.

Another RNAi feeding construct was created by using primers EL23 and EL24 (Table 2) to amplify part of *pezo-1* exon 31 and cloning it into L4440. L4440 was prepared using the Zymogen Miniprep Kit (Irvine, CA) and was then cut with *Eco*RV, which leaves blunt ends. The cut vector was gel purified and treated with shrimp alkaline phosphatase (rSAP) using a kit from NEB (Ipswich, MA). The insert was amplified from *pezo-1* cDNA with the EL23/EL24 primers using the NEB Phusion High-Fidelity PCR Kit (Ipswich, MA). The PCR products were gel purified and cut with the blunt end enzyme *Stu*I. The insert and vector were blunt-end ligated following the NEB Quick Ligation Kit protocol. Ten μL of the ligation mixture was used to transform DH5α cells according to the NEB High Efficiency Transformation Protocol (Ipswich, MA). After incubating for 1 hour at 25°C, 100 μL was plated on an LB-ampicillin selection plate and 900 μL was plated to a separate plate. The colonies were grown over night, plasmid DNA was purified using the Zymogen Miniprep Kit (Irvine, CA) and DNA sequence reads were determined using universal primer M13F(-21). After confirmation that the desired construct was recovered, the plasmid was transformed into the competent HT115 bacterial strain (generous gift of John Ahn and Bill Kelly).

RNAi worm growth plates suitable for RNAi contained NGM media with 1 mM of IPTG and 100 μg/mL ampicillin. HT115 containing the desired recombinant plasmids were streaked onto LB agar plates with ampicillin at a concentration of 50 μg/mL and tetracycline at 12.5 μg/mL and left overnight at 37°C. One colony was inoculated into LB liquid medium with ampicillin, incubated overnight and spotted the next day onto the RNAi worm growth plates. The RNAi plates were kept at room temperature for up to 2-3 days before bacteria was spotted and induced overnight. Four adult hermaphrodites were

placed on an individual plate, which was then incubated at 25°C. Their progeny were fixed, stained and examined under the compound microscope to look at the oocyte nuclear phenotype.

B.3) Results and Discussion

DAPI staining showed that the nonEmo phenotype was only occasionally seen after RNAi under the experimental conditions using *pezo-1*(C10C5.1) and *pezo-1*(T20D3.11) but not in *pezo-1(*EL3/4 insert), irrespective of the worm genotype that was evaluated (Table 1). In contrast, RNAi with the empty L4440 vector (negative control) or *gon-1* vector (positive control) were as expected, showing wild type nonEmo to Emo transition with the empty vector (Figure 10) and full penetrance of the *gon-1* phenotype in all observed worms (Figure 11). Table 1 shows the number of nonEmo oocyte containing gonads that were seen compared to Emo oocyte phenotype containing gonads according to the gene being tested by RNAi. *pezo-1*(exons 1-6) targeted dsRNA to the front part of the transcript while *pezo-1*(exons19/20-21/22) targeted dsRNA to the latter half of the transcript. Originally, these two halves were thought to be two different genes, but later T20D3.11 was found to be part of the same *pezo-1* gene. Due to similarities in the results between using either part of the *pezo-1* gene, it seems that RNAi methods targeting both regions of the *pezo-1* gene should allow knockdown of the PEZO-1 expression. The third experimental condition that used a 165 bp *pezo-1* insert into an L4440 background vector showed no penetrance of the nonEmo phenotype indicating that no knockdown RNAi was successful in any of the strains.

It was more common to see incomplete penetrance of the nonEmo phenotype within one individual worm, seen as either one gonad arm having oocytes with the

nonEmo phenotype (Figure 12, for instance) or in some unique cases with *fer-1* strain there appeared to be gonad arms with both nonEmo and Emo oocytes present closest to the vulva (Figures 14, 16-20). Figures 15, 18, 20, and 21 show what RNAi knockdown of the *pezo-1* transcript looks like when present in both gonad arms. E. J. Gleason initially noted that nonEmo oocytes produced by *pezo-1* mutant strains still transitioned to the Emo phenotype after being laid onto the growth plate. This process is clearly seen in Figures 15, 17, 18, and 21, where the uterus-located oocytes closest to the vulva are nonEmo and show distinctive fluorescent chromosomes while those laid on the growth plate have undergone endomitotic replication. It seems that the laid oocytes furthest from the vulva show the largest amount of DNA replication, suggesting that the transition between the nonEmo to Emo phenotype is, in part, determined by the time an oocyte is outside the animal. This could be due to changes in the environment of the oocyte as it has now exited the gonadal cavity of the hermaphrodite or it could also be linked with an interaction with the vulva muscles as they are squeezed out of the vulva.

When looking at the *rrf-3* strain, there were fewer worms that showed RNAi knockdown of the *pezo-1* gene and so there were fewer gonads with nonEmo oocytes as compared to the other three strains. This is in contrast to what has been published about this strain, where it has been shown to have higher RNAi sensitivity in the gonad than any other strain and greater than wild type RNAi sensitivity in the germline. I observed a low level of response in my feeding-based RNAi experiments for all of the *C. elegans* strains I examined; a 10-30% penetrance amongst RNAi replica experiments has also been seen by other labs [77]. In conclusion, RNAi bacterial feeding experiments confirmed that RNAi of *pezo-1* protein does cause the nonEmo phenotype, confirming

the involvement of C10C5.1 gene with the Emo phenotype. The use of strains *rrf-3* and *eri-1* did not reveal whether or not knockdown of *pezo-1* gene was more effective when in the gonad or in the germline.

C) Creation of a RNAi hairpin construct to selectively target PEZO-1 production in the germline

One unique challenge that RNAi methods face when targeting the germline is that germ cells are more efficient at silencing genes than is the case for somatic cells. Therefore multi-copy transgenes that will be expressed in the soma will not be expressed in the germline. In addition, the role of the 3'UTR is very important in germline cells for specifying particular expression patterns than is the case in somatic cells [84]. It has been shown that embedding transgenes within genomic sequences has facilitated their stable expression in the germline [85]. In order to overcome these challenges, vectors containing specific promoters and 3'UTRs are used to target transgenic expression in the germline.

In order to target short hairpin RNA (shRNA) specifically in the germline of *C. elegans*, the *pie-1* promoter and 3'UTR were used to drive expression throughout the germline. The *pie-1* promoter is able to drive expression in all germline cells, but pairing the promoter with the *pie-1* 3'UTR drives expression in oocytes and embryos [86, 87]. By placing a *pezo-1* hairpin construct between the *pie-1* promoter and 3'UTR and using this construct to create transgenes, specific targeted expression of the shRNAi in oocytes and embryos should occur. A shRNA-expressing transgenic construct should, in principle, be a more stable source of shRNA in the germline than feeding or any other way of RNAi delivery [88].

C.1) Methods

We designed 3 sets of primers that would amplify three different exon regions from the *pezo-1* gene that are present in all of the 12 alternatively spliced RNA species. (Figure 3; Table 2). By placing the inserts in a forward and then reverse direction, a hairpin mRNA transcript would form after transcription (Figure 23, left). First, RT-PCR was used with cDNA from N2 and *him-8* strains to isolate the inserts using the primers described in Table 1. The cDNA was prepared (as above in section B), and the inserts were cut with *Bam*Hi-HF and *Spe*I, gel purified using a 1% gel with ethidium bromide staining and DNA was recovered with a Zymogen DNA Gel Clean Kit (Irvine, CA). The *pie-1* promoter and 3'UTR were in vector pHF10, which was provided by H. Furuhash and W. G. Kelly. The vector was then grown overnight in LB-ampicillin liquid medium and prepared using the Zymogen Miniprep kit (Irvine, CA). This vector was digested with restriction enzymes *Bam*Hi-HF and *Spe*I and gel purified.

The inserts were originally placed in a triple ligation reaction and transformed into SURE 2 competent cells (from Agilent Technologies; Santa Clara, CA) however restriction digestion and sequencing showed that the inserts were not properly cloned in the pHF10 backbone. SURE (Stop Unwanted Rearrangement Events) 2 competent cells are more tolerant of recombinant constructs that have repeated sequences because they are restriction minus (McrA-, McrCB-, McrF-, Mrr-, HsdR-) endonuclease (endA) deficient, and recombination (recB recJ) deficient with a lacIqZΔM15 gene, on the F′ episome, that allows blue white screening. In *Escherichia coli* there are two types of restriction-modification systems and one kind directs endonuclease cleavage towards DNA targets that have specific methylation of certain sequences. McrA and McrCB are

two methyl-cytosine restricting systems while Mrr is a methylated adenine recognition and restriction system. HsdR is a gene that is part of the second type of restriction-modification system, where along with hsdM and hsdS genes, a multimeric enzyme that cleaves or methylates particular target sequences is active. With these two restriction-modified systems mutated and unable to protect the bacteria from breaking down foreign DNA, this cell line should have allowed the cloning of the plasmid containing the hairpin structure better than the regular DH5α line [89] [90, 91].

Due to difficulties in confirming the hairpin inserts by DNA sequencing, a step-by-step approach was taken by first ligating the reverse insert isolated with primers EL3 and EL4 into the vector using the enzymes *Bam*Hi-HF and *Spe*I and then the forward insert was ligated into the vector already containing the reverse insert by using *Stu*I, a blunt cutter, after isolating the forward insert through PCR using primers EL23 and EL24. Sequencing results confirmed that both a forward and a reverse 164 bp fragments are in the pHF10 vector, creating a 328 bp long hairpin insert (Figure 23).

C.2) Results

This vector is now ready to be injected into OD95 *fer-1(b232ts) I*; *ltIs37 IV; ltIs3* with pPD118.20 which contains *myo-3* GFP or pPD118.33 which contains *myo-2* that confers fluorescence to the body wall and pharyngeal muscle, respectively. In order to ensure RNAi hairpin specificity one could perform the injection in a *sid-1* mutant background so that the dsRNA is unable to spread throughout the worm body and will stay in the germline. My repeated bacterial transformation failures indicates that, perhaps, the SURE 2 Competent cells are not able to tolerate recombinant plasmids that contain inserts encoding a RNAi hairpin structure.

Chapter 5: Creation of a *pie-1::sid-1::pie-13* expression clone to enhance RNAi in the germline

A) Introduction

The *sid-1* gene is a transmembrane protein that is essential for the spreading of systemic RNAi. Calixto et al (2010) [92] showed that expressing *sid-1* under the control of a neuron-specific promoter created worms that had enhanced RNAi sensitivity for neuronally expressed genes that had been resistant to RNAi in wild type worms. By creating a vector with the *pie-1* promoter and *pie-1* 3'UTR controlling expression of a *sid-1* insert, we hoped that using it to create a transgenic line would allow more effective feeding-based RNAi for genes whose loss of function causes a spermatogenesis-defective (*spe*) phenotype.

B) Methods

The TU867 vector containing the *sid-1* genes was ordered from Addgene (Cambridge, MA) and grown overnight in LB medium with ampicillin at 37°C. The next day plasmids were prepared using Zymogen Miniprep Kit (Irvine, CA) and digested using *Bam*HI-HF and *Sna*BI. The *sid-1* insert was gel purified, cleaned with the appropriate Zymo Gel Clean Kit (Irvine, CA) and blunt-ended using the Thermo Fisher Scientific Fast DNA End Repair Kit (Waltham, MA). In the same way that pHF10 vector was prepared to create the RNAi hairpin, the vector was cut with *Stu*I and rSAP was used to phosphatase the ends of the cut vector. These recombinant plasmids were ligated, transformed into DH5α cells, grown overnight and miniprepped using the Zymogen kit (Irvine, CA).

C) Results

Sequencing and restriction digest results have been unable to confirm that the *sid-1* gene is properly inserted into the pHF10 vector. Transformation appeared to be successful with more colonies growing on the experimental plates than the negative control plates. However, the inserts were of varying lengths, suggesting that this is 16 kb plasmid was unstable and subject to deletion. Several attempts to ligate and transform this vector were unsuccessful. I am working out different methods to confirm that the *sid-1* portion has been successfully inserted, and that it is in the correct orientation.

D) Discussion

The creation of a vector with the *sid-1* gene between the *pie-1* promoter and *pie-1* 3'UTR might make RNAi more consistent for studies of spermatogenesis, oogenesis, and fertilization in *C. elegans.* As was shown by the Chalfie lab, having SID-1 in the plasma membrane of neurons can facilitate RNAi of neuronally-expressed genes using a feeding assay [93]. They hypothesized that wild-type neurons must have a low level of SID-1 or an equivalently functioning protein that regulates spreading of dsRNA. By analogy to the Chalfie experiments, we hypothesized that expression of *sid-1* in the germline would improve response to RNAi methods. If this were to work in the germline as envisioned, it would be a significant help for future studies because it would make RNAi more consistent and might allow the sort of large-scale screens that have been performed for somatically-expressed genes to be applied to genes with germline functions. For instance, by utilizing the Ahringer RNAi feeding library to feed a *C. elegans* line with fluorescently tagged PGL-1 RNA binding protein, the genes that are involved with P granules in *C. elegans* were discovered [94]. Another study used genome-wide studies to

identify novel genes that are associated with longevity in *C. elegans* using an RNAi sensitive strain [95]. In addition, other research has shown that expression of SID-1 in the silkworm *Bombyx mori*, has greatly facilitated the uptake of dsRNA *in vitro* into ovary-derived Bmn4 cells *[96]*. Similarly, with the creation of a transgenic *C. elegans* line expressing *sid-1* in the germline, we could perform a genome-wide screen of genes in order to identify those that participate in germline development and gametogenesis [97].

Chapter 6: Conclusions and Future Directions

By creating several strains with different properties, I was able to show that loss of function for the C10C5.1 gene is the exclusive cause of the novel Emo phenotype I have characterized. Genetic analysis by Reinke and Cutter (2009) showed that most *C. elegans* operons are germline expressed and that genes involved in spermatogenesis are rarely found in operons [98]. Consistent with prior observations, C10C5.1 is the only gene within the CEOP4328 operon that is associated with the Emo phenotype, while the other three genes within the operon have apparently unrelated functions [99]. The fact that operons are expressed mainly in the germline suggests that this transmembrane protein could be expressed in *C. elegans* oocytes. In addition, I have created vectors that will allow RNAi methods that specifically target expression in the germline. By using the OD95 *fer-1(b232ts)*I; *ltIs37*IV*; ltIs3* we should be able to further investigate our hypothesis that knockdown of *pezo-1* expression in the germline is determining the transition from nonEmo to Emo phenotype in ovulated oocytes.

The heterogeneity of RNAi results within the two gonadal arms of an individual worm also suggests that there might be some barriers affecting spreading of RNAi between the two arms; this unusual phenomenon was also observed for *pezo-1* by K. Pohl

[43]. In addition, RNAi penetrance was similar amongst all examined strains, including the RNAi hypersensitive strains *rrf-3* and *eri-1,* despite the greater *rrf-3* sensitivity to RNAi in gonads. Despite *rrf-3* and *eri-1* strains being more sensitive than wild type in the germline, there does not seem to be any apparent outstanding penetrance in these two strains in comparison with *fer-1* or OD95 *fer-1(b232ts) I*; *ltIs37 IV; ltIs3*.

Prior work has shown that *rrf-1* is differentially sensitive to RNAi against genes expressed in the germline but not in the soma. More specifically *rrf-1* mutants were shown to be sensitive in some somatic tissues to RNAi, but were resistant to *gfp* RNAi in the somatic gonad. RRF-1 is a one of the RdRPs that amplifies dsRNA triggers in the exogenous siRNA pathway that acts in the somatic tissue [100]. If there was greater or decreased penetrance in this strain, then it would help to verify that it is either the gonad or germline expression of PEZO-1 that causes the Emo phenotype. Similarly, creating a strain that uses GFP-tagging of the PEZO-1 protein in an OD95 *fer-1(b232ts)*I; *ltIs37*IV*; ltIs3* background should allow visualization of PEZO-1 and other aspects of the oocyte.

Following the work performed by E.J. Gleason, RT-PCR could be used to analyze *glp-1,* which is a strain that has a germline deficiency. Loss of *glp-1* has the same effect on germline proliferation as eliminating the distal tip cell, which controls the transition from mitosis to meiosis of the germline [101]. Typically, the maturing germ cells exit mitosis and enter meiosis when they move into the proximal end of the gonad, while the primordial germ cells near the distal tip cell remain mitotically active through adulthood (Figure 2) [102]. *glp-1* mutants produce a small population of primordial germ cells that all immediately enter meiosis and precociously become 4-8 sperm-like cells. Therefore, the somatic gonad is morphologically intact while there is a greatly diminished germ line

[103]. By using the same RT-PCR tactics (described in Chapter 1) to look at whether *pezo-1* RNA transcripts are expressed in *glp-1* mutant strains, we should be able to see whether *pezo-1* transcription happens in the absence of the germline.

Because the C10C5.1 transcript was expressed in strains only expressing either oocytes or sperm, and in hermaphrodite and male gonads we can conclude that C10C5.1 is being expressed in all types of gonads but its expression in germline cells remains uncertain. In wild-type strains, worms that are sterile at 25˚ will show the gradual appearance of the Emo phenotype due to further endomitotic replication of the DNA as the oocyte progresses closer to the vulva in a linear and timely manner. This transition occurs after the ovulated oocyte has not been fertilized and passes through the spermatheca. Oocytes are paused in meiosis prior to ovulation but meiosis resumes once they are in the spermatheca and are fertilized. However, once oocytes are unfertilized for a prolonged period of time, they start to exhibit the Emo phenotype [104]. Having an active PEZO-1 transmembrane protein may allow the oocyte to prepare for fertilization by mechanical activation of an as yet uncharacterized signal transduction pathway that drives the transition from meiosis to mitosis. The fact that oocytes produced by loss of function *pezo-1* mutants can still be successfully fertilized indicates that activating this signal transduction pathway is not essential.

Oocyte passage through the spermathecal valve and/or the vulva could potentially interact with the mechanosensory PEZO-1 channel protein if it is a transmembrane protein in the oocyte plasma membrane. There may be an interaction between the oocyte and its transitioning to new environments or new pressures that signal to the nonEmo oocyte to maintain or cause transition to the Emo phenotype. Further investigations as to

the internal environment of the gonad would help clarify this process and how we could maintain the signal of remaining nonEmo even after oocytes have been extracted from the gonads. One way this could be done is to analyze the mechanisms of how the oocytes are endocytosing yolk and to see that if extruded nonEmo oocytes are treated with inhibitors that block those receptors or are placed in environments where they have access to a similar type of material that they will be able to remain paused in meiosis [105]. While my results are not conclusive, it seems probable that PEZO-1 is expressed in the plasma membrane of the oocytes and is regulating the Emo phenotype.

Figures and Reference

	Gene Knockdown				
strain	*pezo-1*(exons1-6)	*pezo-1*(exons19/20-21/22)	*pezo-1(EL3/4 insert)*	L4440 (negative)	*gon-1* (positive)
rrf-3	14/66	5/10	0/20	0/12	0/12
OD95 *fer-1*	15/78	5/24	0/20	0/12	0/12
fer-1	8/32	4/10	0/20	0/10	0/10
eri-1	4/42	1/8	0/20	0/10	0/8

Table 1. RNAi penetrance in tested strains. There were similar results seen when feeding RNAi was performed with either the C10C5.1(exons1-6) and C10C5.1(exons19/20-21/22) portion of *pezo-1*. Penetrance was seen in all gonads for the *gon-1* phenotype while no penetrance was seen with feeding empty L4440 or with the 165bp EL3/4 insert. Data are expressed with # with the expected phenotype / # of gonad arms examined.

Primer Pair	Exon	Length (bp)
EL1/2	20	264
EL3/4	31	165
EL7/8	27-29	1644

Table 2. Regions of C10C5.1 used for RNAi hairpin constructs. Three sets of primer pairs (left column) were designed to amplify different exon regions of C10C5.1 (middle column) that were present in all of the alternatively spliced variants encoded by the *pezo-1* gene. The length of the amplified PCR product is also noted (right column).

Primers	Sequence (5' - 3')	Insert
EJG108	CACTGCTTGCAGCTGCCATAATCC	exon 1/2 forward
EJG109	GAGAGAGCCCATGTCATCATAGCAGTC	exon 9/10 reverse
EJG110	GACTGCTATGATGACATGGGCTCCTC	exon 9/10 forward
EJG111	GAAATAGGGCTCCCGATTCACCG	exon 15 reverse
EJG112	CGGTGAATCGGGAGCCCTATTTC	exon 15 forward
EJG113	GCTAACAAAGTCAATAGTGAGTAGTAGTGG	exon 1 i and j splice variants forward
EJG114	GGAATACACATCCAAATATTTGAAGGCAAAC	exon 19/20 reverse
EJG115	GTTTGCCTTCAAATATTTGGATGTGTATTCC	exon 19/20 forward
EJG116	GCAGCGTACATTATCTGTCCAGGATC	exon 26/27 reverse
EJG117	GATCCTGGACAGATAATGTACGCTGC	exon 26/27 forward
EJG118	GGAATGGAATATTCATGAATACTTTGAATGCAATC	exon 29/30 reverse
EJG119	GATTGCATTCAAAGTATTCATGAATATTCCATTCC	exon 30 forward
EJG120	GTGTCTCGTGTCGTGTAACTATCCG	exon 30 reverse
EL1	tgcggccgcactagtcctcaggggatcctcaATGCTGGGACTTCCTG	EL1/2 insert

	AATCGATGC	forward
EL2	taggcctgaattcAAAGAACTGAAGTGGATACAGAATCG	EL1/2 insert reverse
EL3	tgcggccgcactagtcctcaggggatcctcaATGACCTTGAATCTCG AACAAGGAAAATC	EL3/4 insert forward
EL4	taggcctgaattcTGGGAATGCTCTATCAATAAATCCG	EL3/4 insert reverse
EL7(EJG 117)	tgcggccgcactagtcctcaggggatcctcaATGGATCCTGGACAGA TAATGTACGCTGC	EL7/8 insert forward
EL8(EJG 118)	taggcctgaattcGAATGGAATATTCATGAATACTTTGAAT GCAATC	EL7/8 insert reverse
EL23	cgaaggccttcaATGACCTTGAATCTCGAACAAGGAAAAT C	EL3/4 insert forward
EL24	gataggcctcctaagTGGGAATGCTCTATCAATAAATCCG	EL3/4 insert reverse

Table 3. Primers used for PCR. Lower case letters are parts of the primer that facilitated cloning and restriction digestion and are not found in *C. elegans* DNA sequence.

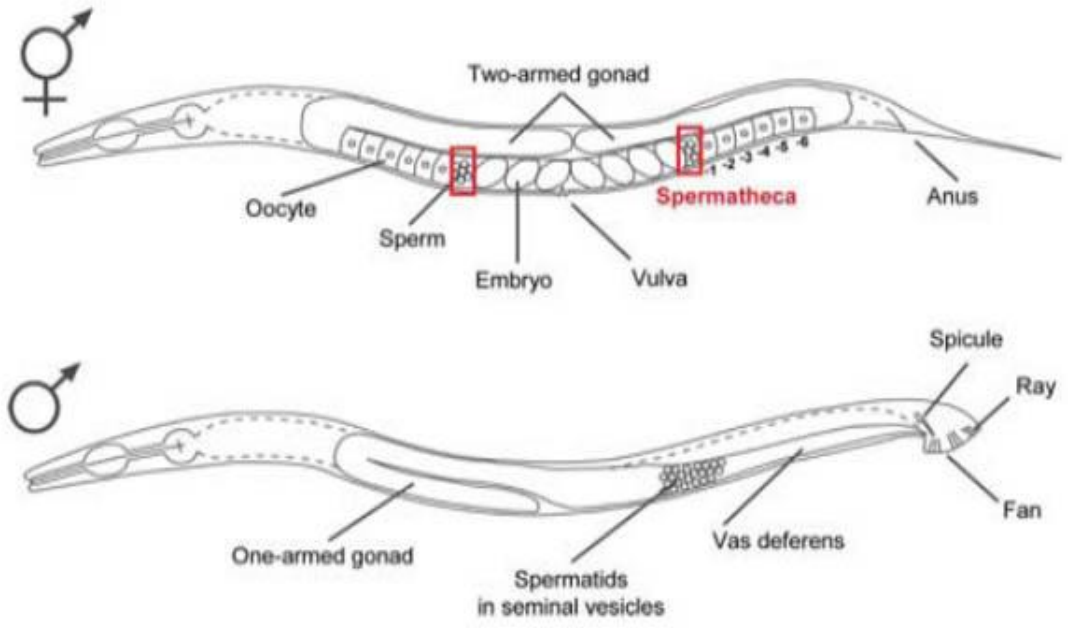

Figure 1. Reproductive anatomy of *C. elegans* hermaphrodite and male is shown above. The hermaphrodites have a bilobed gonad that includes a spermatheca where the oocytes are fertilized by sperm and eventually extruded through the central opening called the vulva. Modified from [24].

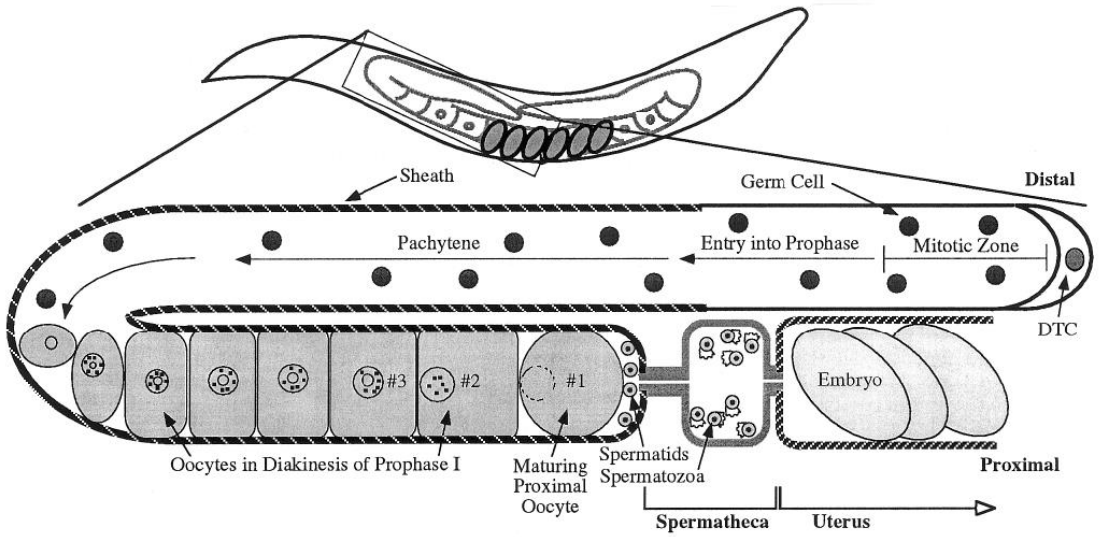

Figure 2. One of the two-arms in the hermaphrodite gonad. Germ cells progress from the distal tip and develop into oocytes that are paused in diakinesis of prophase I before reaching the spermatheca. In the spermatheca the sperm are waiting for a mature oocyte to enter and, after being fertilized, the embryo will be squeezed into the uterus and then extruded by the vulva. Taken from [15]

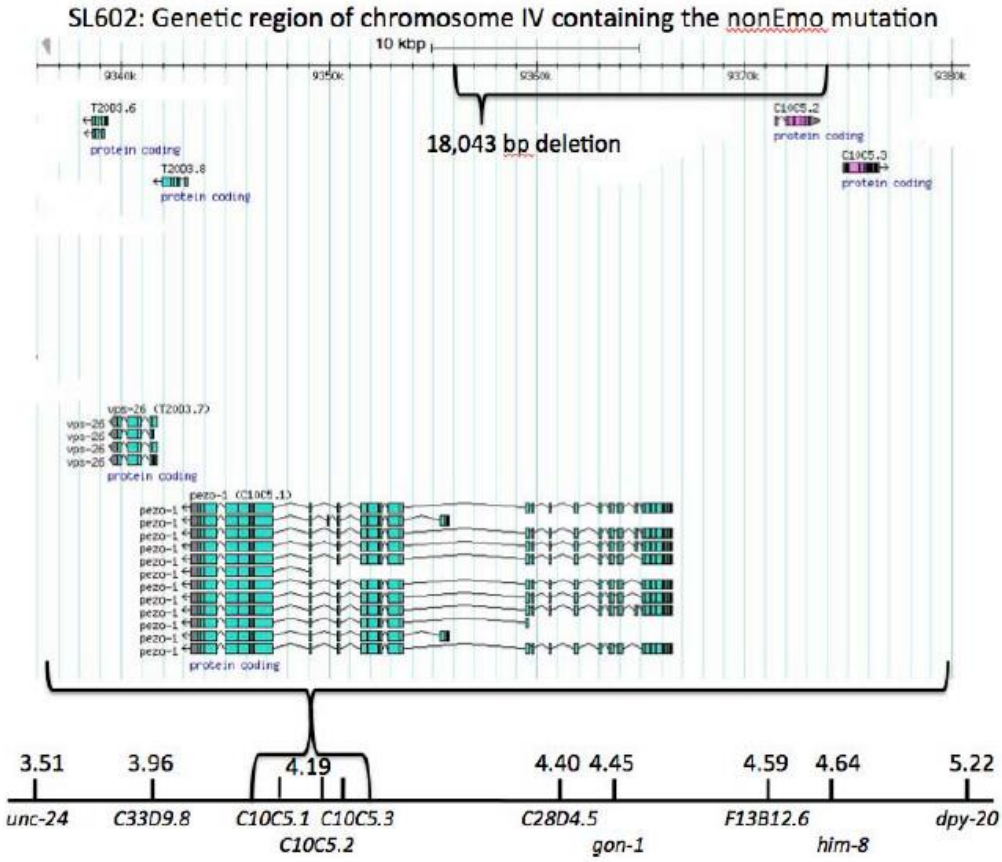

Figure 3. Genetic mapping of chromosome IV containing the nonEmo mutation in strain SL602 *unc-24(e138) him-8(e1462)*IV. 18,043 bp deletion was found in the region of the CEOP4328 operon containing *vps-26*, C10C5.1, C10C5.2, and C10C5.3. There were four other point mutations in C33D9.8, C28D4.5, *gon-1*, and F13B12.6. Modified screenshot from www.wormbase.org

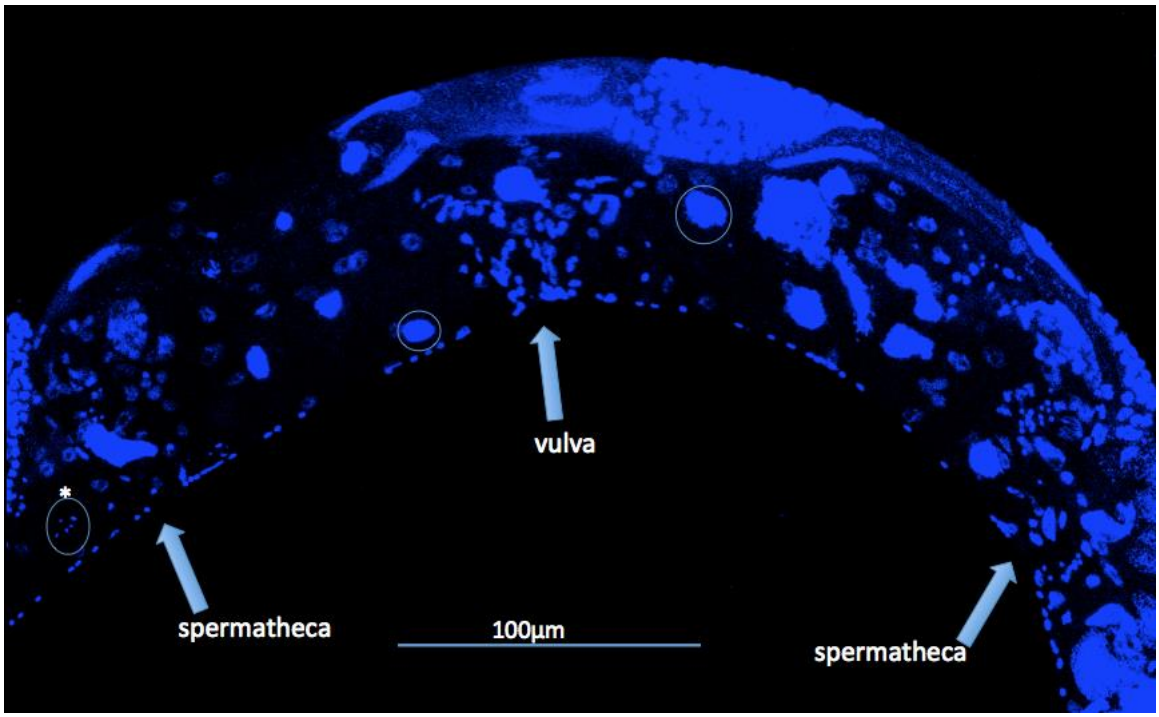

Figure 4. An Emo phenotype is shown by the T20D3.7*(gk773646); fer-1* double mutant. In this figure, the oocyte DNA has been visualized by DAPI staining. In the two arms of the gonads, that extend left and right from the vulva, the oocytes show an Emo phenotype (circled on either side), represented by one large blue bright spot, rather than seeing six small blue dots indicating individual chromosomes that are seen when worms exhibit the nonEmo phenotype (marked with a *; circled before the spermatheca).

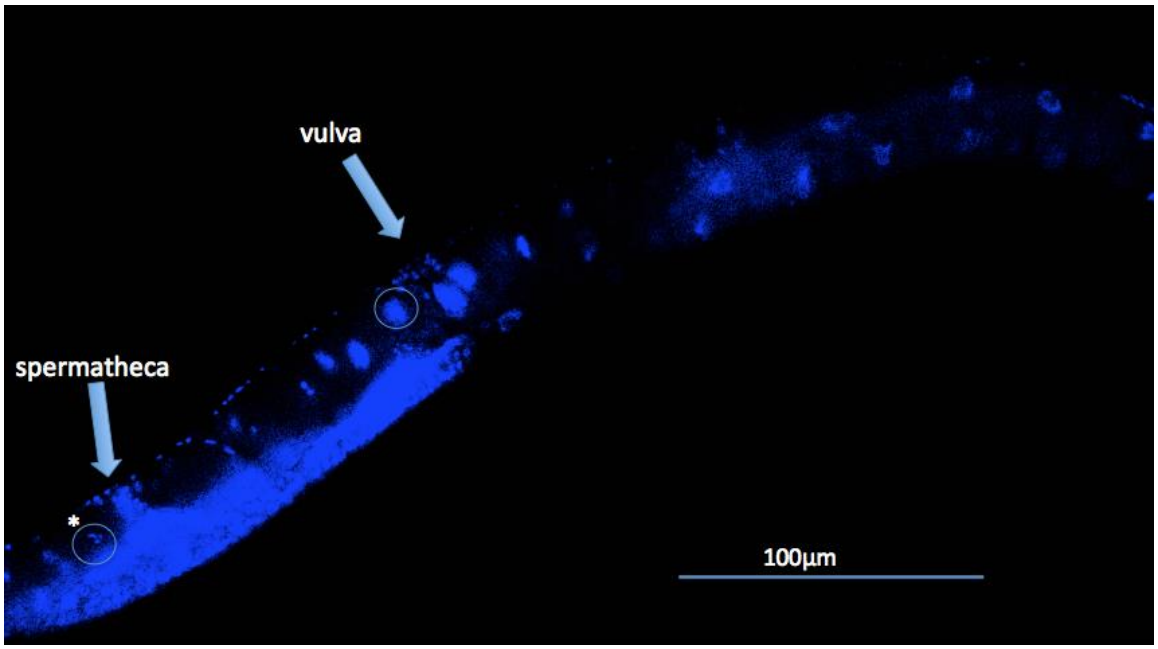

Figure 5. An Emo Phenotype is shown by the T20D3.8*(gk208783); fer-1* double mutant. In this figure, the oocyte DNA has been visualized by DAPI staining. In the two arms of the gonads, that extend left and right from the vulva, the oocytes show an Emo phenotype (circled on either side), represented by one large blue bright spot, rather than seeing six small blue dots indicating individual chromosomes of nonEmo phenotype (marked with a *; circled before the spermatheca).

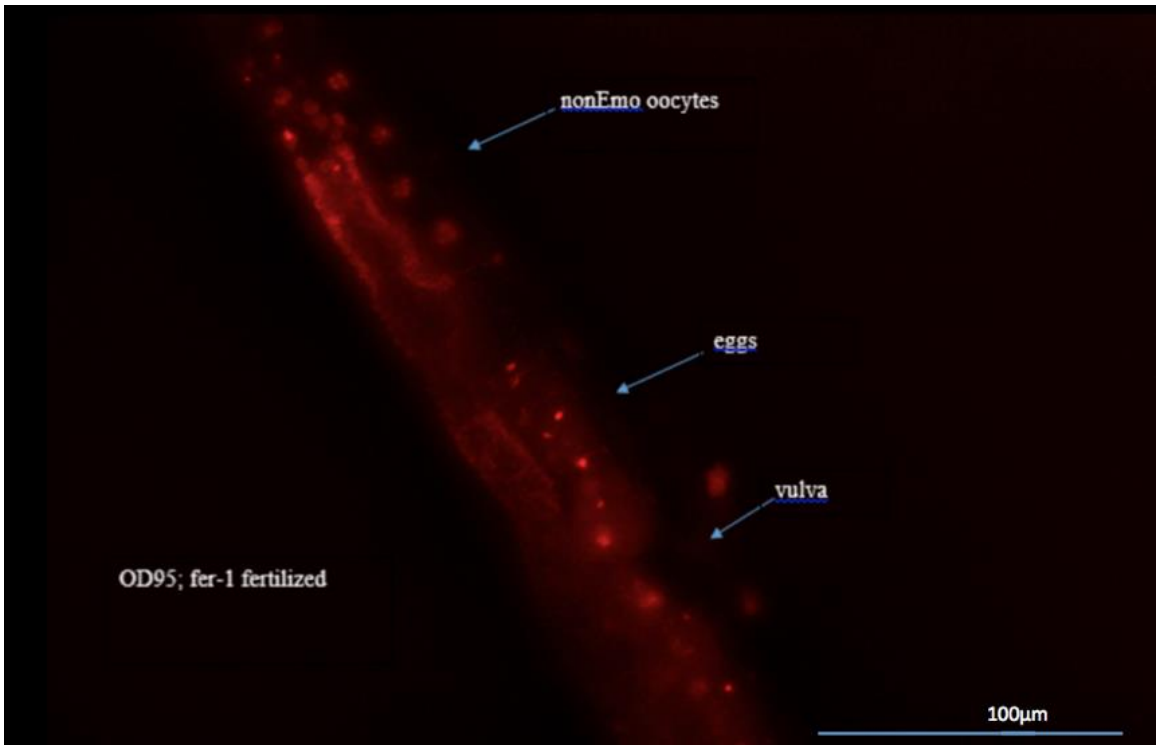

Figure 6. OD95 *fer-1(b232ts)*I; *ltIs37*IV*; ltIs38*. Before the spermatheca you can see the nonEmo oocytes labeled and as they progress past the spermatheca towards the vulva, the oocytes are fertilized and become eggs, which have a distinctive, condensed nuclei in red. Nuclei shown by mCherry fluorescence; 20X, 25°C. n=4.

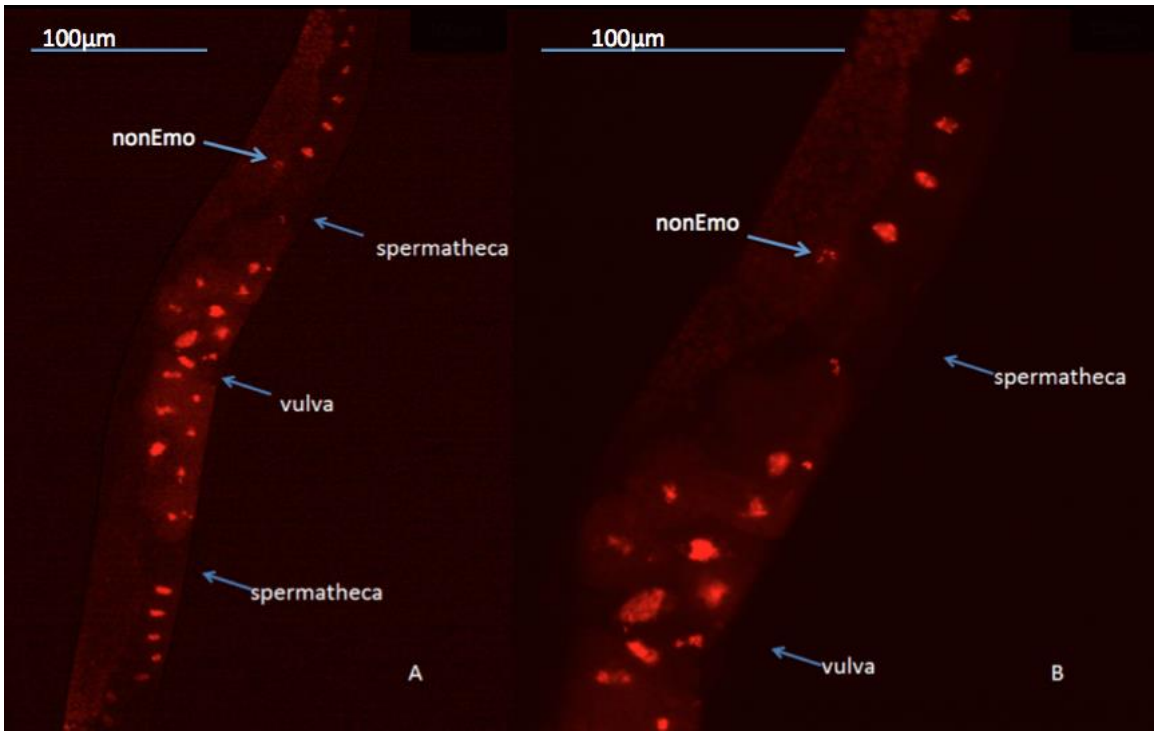

Figure 7. OD95 *fer-1(b232ts)*I; *ltIs37*IV*; ltIs38*. In panel A, the symmetric nature of the mirror-image bilateral gonads is evident. In panel B, the transition from distinctive red dots that characterize the nonEmo phenotype signifying distinct chromosomes (above the spermatheca in this panel) while the oocytes are showing the Emo phenotype after they get close to the vulva. Nuclei shown by mCherry fluorescence; 20X, 25°C. n=4.

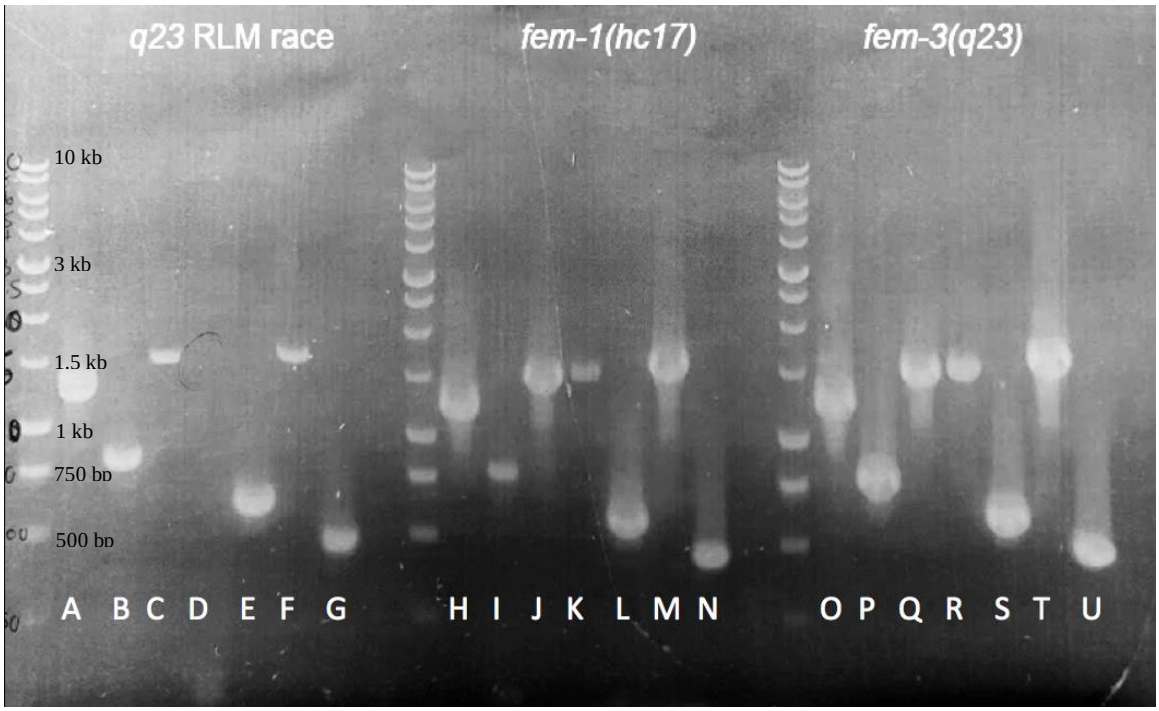

Figure 8. Expression of *pezo-1* RNA transcripts. (by E. J. Gleason). The left-most section shows RLM-RACE results. Seven primer pairs were used to amplify cDNA from full-length capped mRNA. From left to right, the amplified regions were amplified were: (A, H, O) from exon 1/2 to exons 9/10, (B, I, P) exon 9/10 to exon 15, (C, J, Q) exon 15 to exon 19/20, (D, K, R) exon 1 of I and J splice variants to exon 19/20, (E, L, S) exon 19/20 to exon 26/27, (F, M, T) exon 26/27 to exon 29/30, and (G, N, U) a region of exon 30. You can see that in lane D, the fourth primer pair from exon1 of the *pezo-1* i and j splice variants did not work. Because it was not amplified by the RLM-RACE Kit, this indicates that the mRNA was either not present or that it is not a full-length and 5' capped mRNA. Again when using the primers, the transcript was absent in both strains which indicates that this splice variant might not be present. From lanes H-N you can see the results of using RT-PCR to amplify those same regions in feminized *fem-1(hc17)* while lanes O-U show the results from masculinized *fem-3(q23)*.

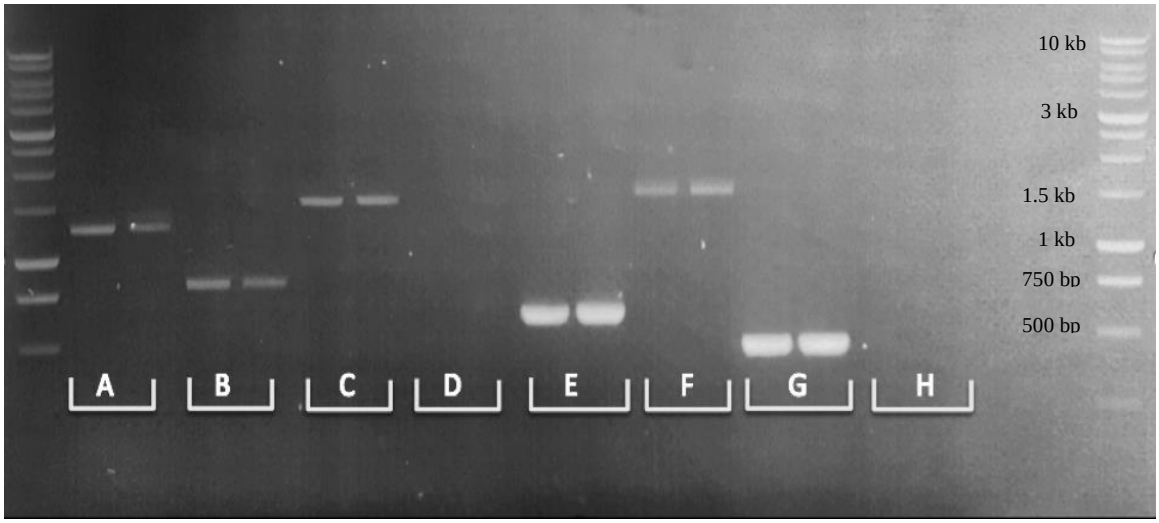

Figure 9. RT-PCR performed on N2 hermaphrodites and *him-8* males by E. J. Gleason. Each pair of lanes from left to right shows the same exon transcript. The left-most band is the RT-PCR products amplified from the hermaphrodites and the right-most band of each pair shows amplified DNA from males. All tested exon transcripts are present in both hermaphrodites and males using the same exon regions shown in Figure 8. As for Figure 8, there is no amplification of the primers in lane D, which should amplify exon 1 of the splice variants I and J. Lane H was the negative control for the PCR reaction using only primer and no template DNA.

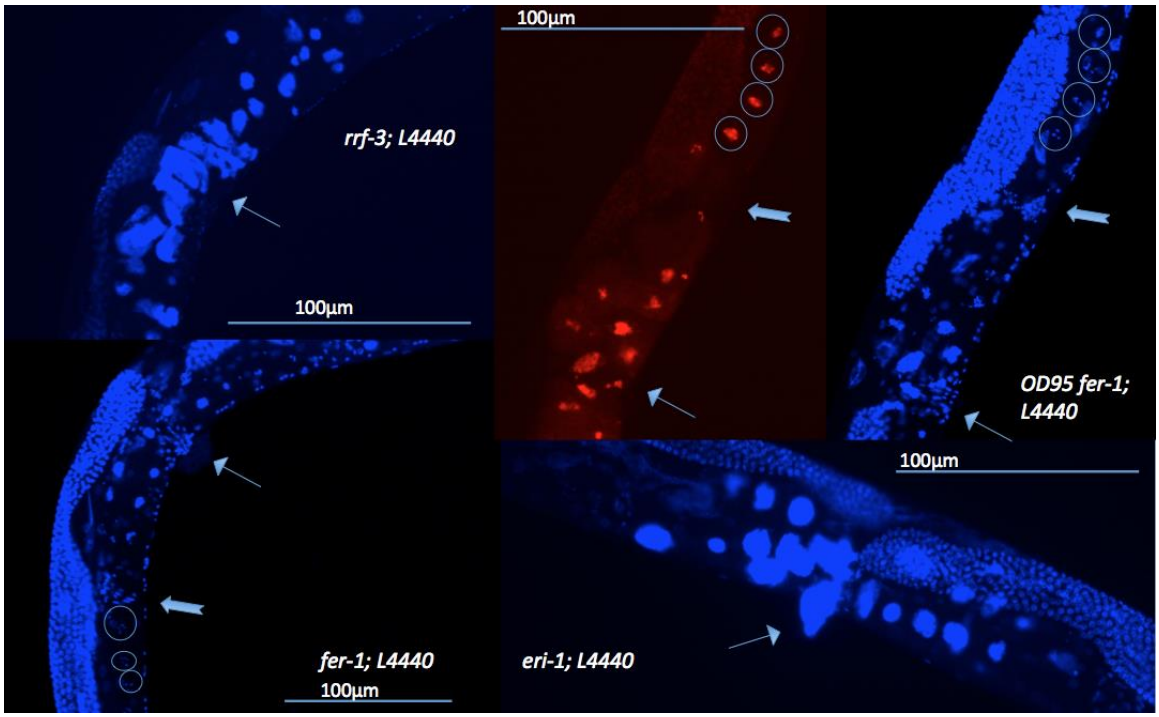

Figure 10. RNAi bacterial feeding of empty L4440 vector (negative control). The skinny arrow points to the vulva, while the thicker arrows indicate the spermatheca. The nonEmo oocytes are circled before the spermatheca. All strains showed a transition from the nonEmo to the Emo phenotype after passing through the spermatheca. Nuclei are stained with DAPI; 20x, 25°C. n=5 for *rr-3* and OD95 *fer-1(b232ts)*I; *ltIs37*IV*; ltIs38* strain. n=5 for *fer-1* and *eri-1*.

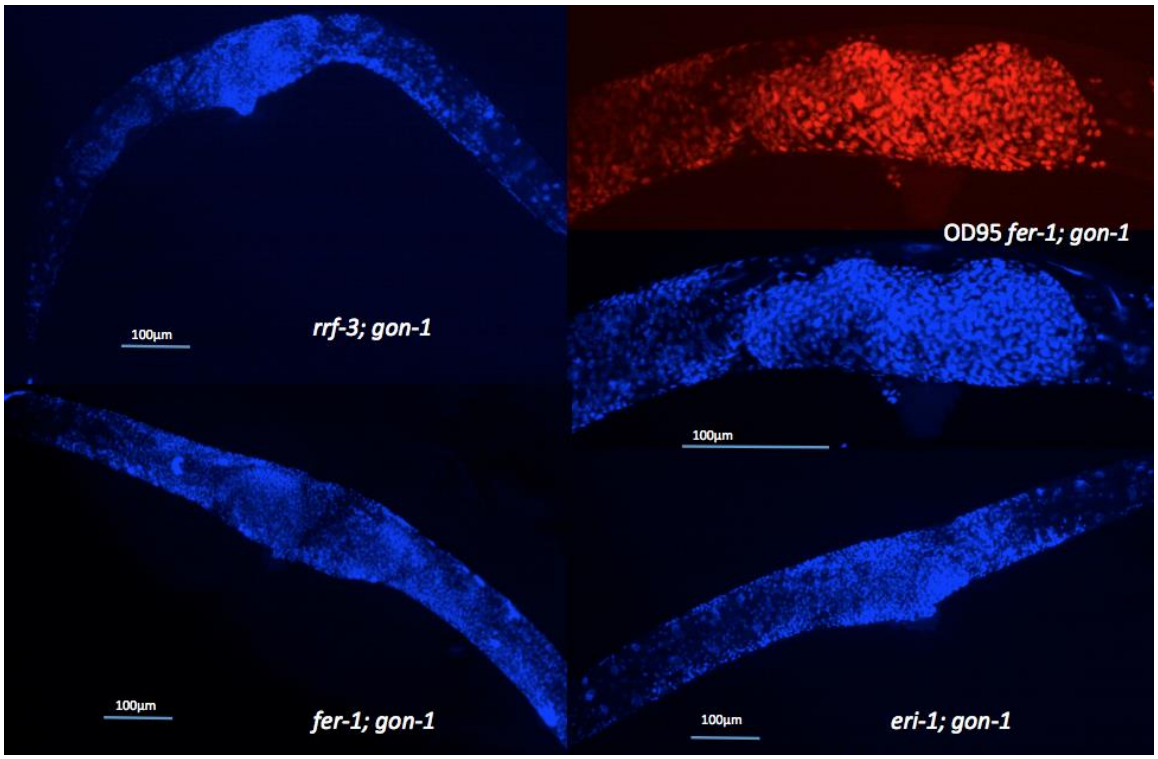

Figure 11. RNAi bacterial feeding with *gon-1* in all strains as indicated above. When RNAi knockdown of *gon-1* is present the above phenotype is shown with irregular gonad morphology with a bloated central area in the worm. Nuclei are stained with DAPI; 20x, 25°C. n=5 for *rr-3* and OD95 *fer-1(b232ts)*I; *ltIs37*IV*; ltIs38* strain. n=6 for *rrf-3* and OD95 *fer-1(b232ts)*I; *ltIs37*IV*; ltIs38* strain. n=5 for *fer-1*. n=4 for *eri-1*.

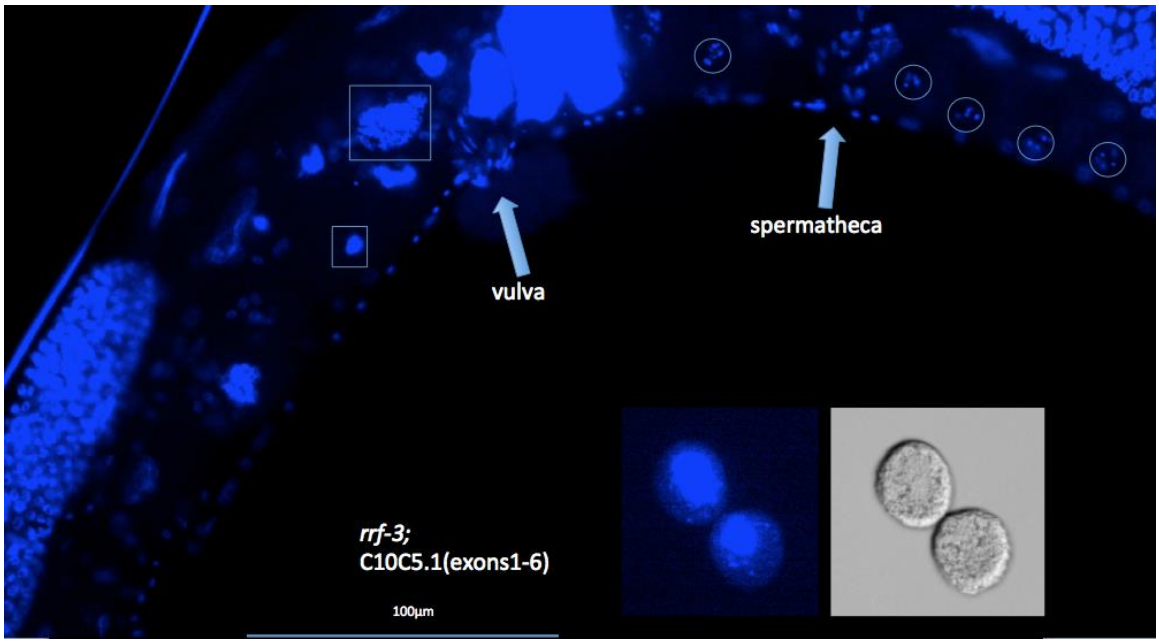

Figure 12. Testing C10C5.1 (exons1-6) RNAi by a bacterial feeding assay in the *rrf-3* strain. In four worms, there were nonEmo oocytes in the uterus (circled) with the presence of Emo oocytes towards the vulva in the other gonad arm (squares). The inset shows a DIC picture of laid oocytes, which appear to the left in the DAPI image. Nuclei stained with DAPI; 20x, 25°C. n= 33.

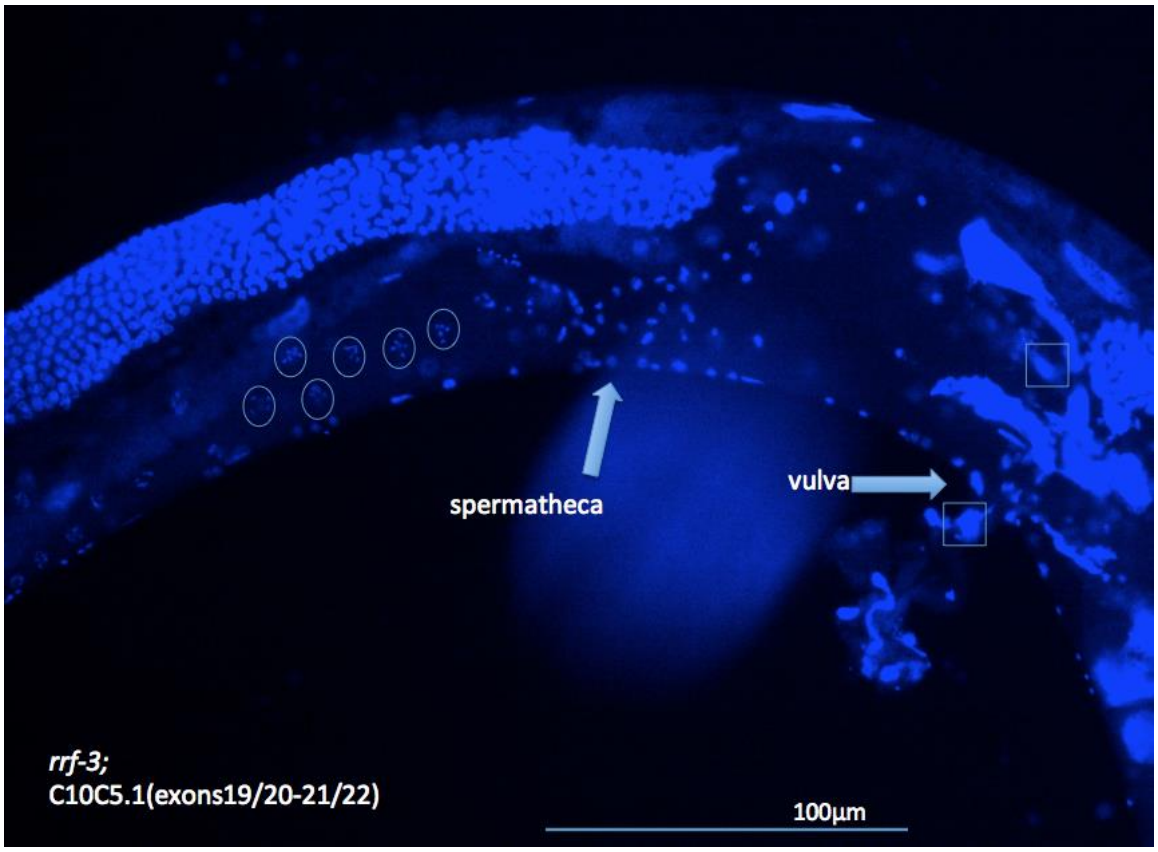

Figure 13. RNAi bacterial feeding with C10C5.1 (exons19/20-21/22) in the *rrf-3* strain. C10C5.1 (exons19/20-21/22) targets the 3' end of the *pezo-1* RNA transcript. Oocytes prior to ovulation show clear meiotic chromosomes (circled). All worms were found to have Emo gonads shown by the presence of Emo phenotype oocytes (boxed). Nuclei stained with DAPI; 20x, 25°C. n=

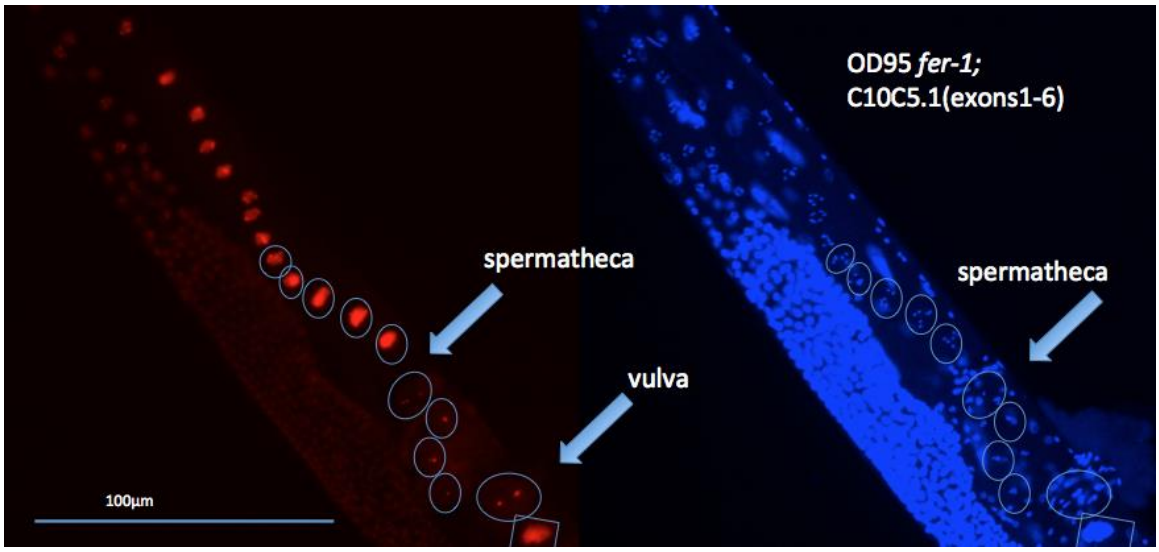

Figure 14. RNAi bacterial feeding with C10C5.1 (exons 1-6) in the OD95 *fer-1(b232ts)*I; *ltIs37*IV*; ltIs38* strain. Two worms showed nonEmo oocytes in one of the gonad arms, shown above with one imaged live for mCherry (left) and the same worm fixed and stained with DAPI to visualize nuclei (right); 20x, 25°C. n=39.

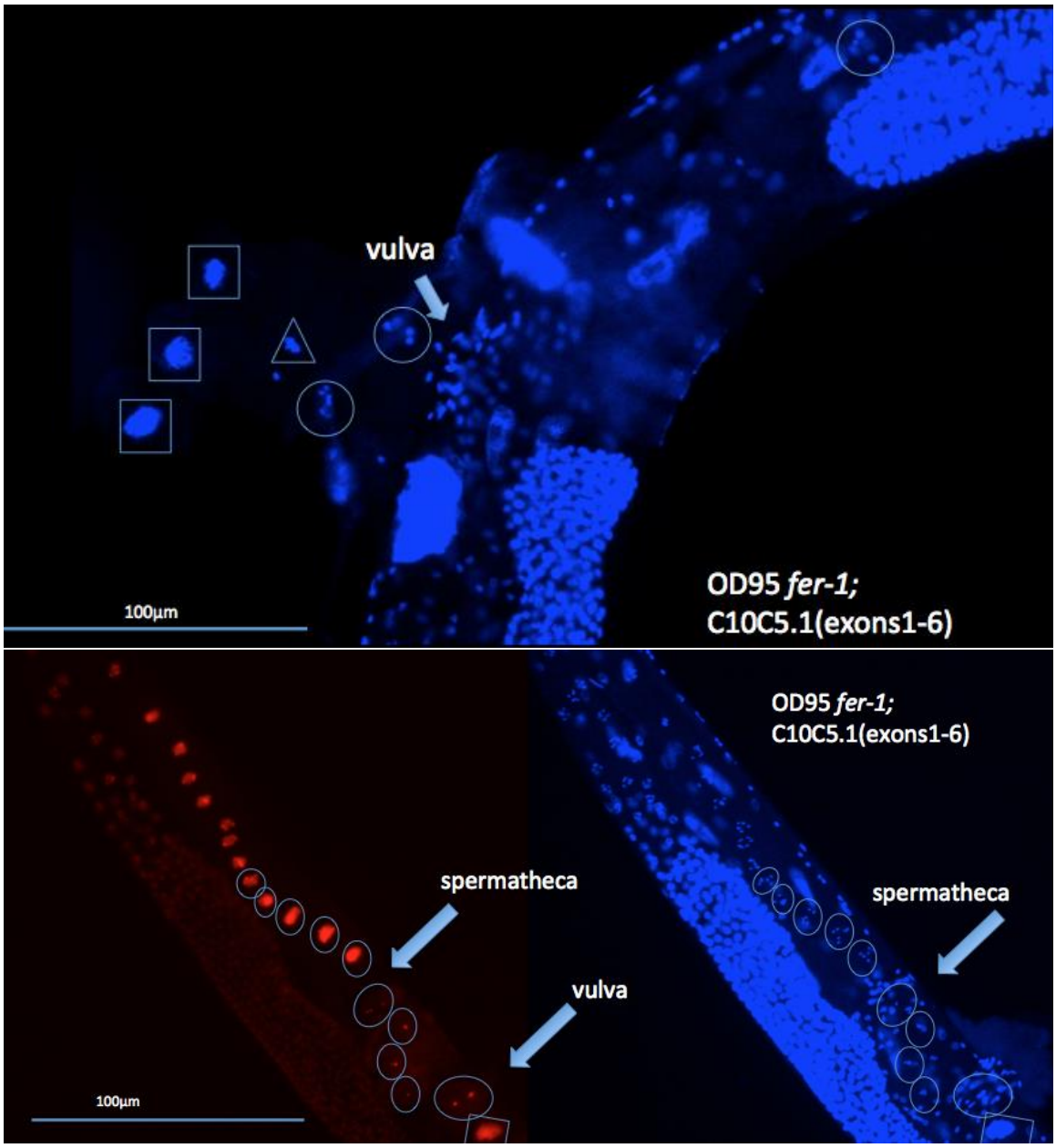

Figure 15. RNAi bacterial feeding with C10C5.1 (exons1-6) in the OD95 *fer-1(b232ts)*I; *ltIs37*IV*; ltIs38* strain. Three worms showed nonEmo oocytes in both of the gonad arms. Oocytes that have been most recently laid are still nonEmo (circled) while the ones farthest from the vulva are Emo (boxed) and a transitional oocyte is also evident (in a triangle). Nuclei stained with DAPI; 20x, 25°C. n=39

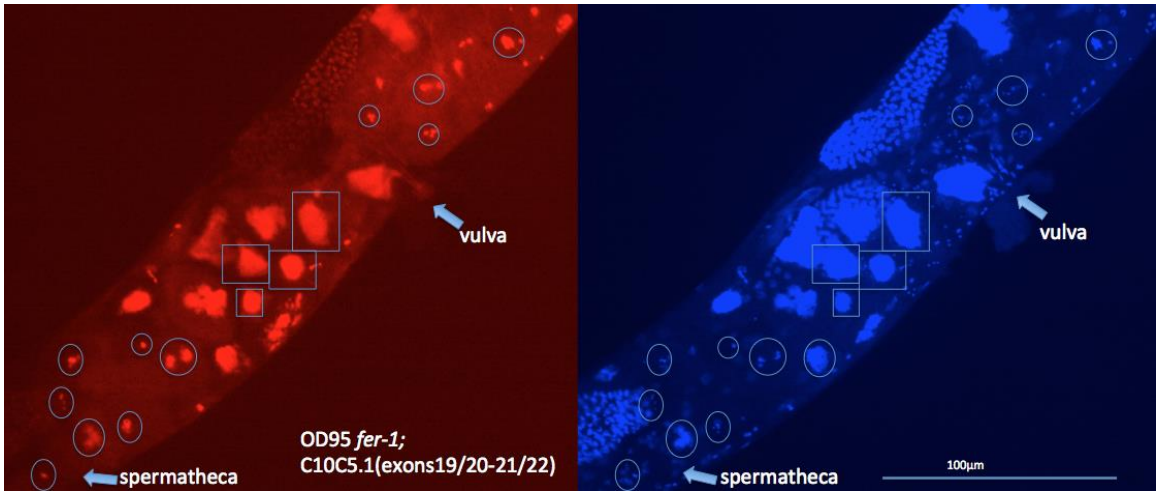

Figure 16. RNAi bacterial feeding with C10C5.1 (exons19/20-21/22) in the OD95 *fer-1(b232ts) I*; *ltIs37 IV; ltIs38* strain. Four worms showed that one gonad arm had the nonEmo phenotype (circled) while the other arm had Emo oocytes (boxed). The panel on the left shows mCherry visualization of chromatin and the matched panel on the right shows DAPI staining of DNA. 20x, 25°C. n=24.

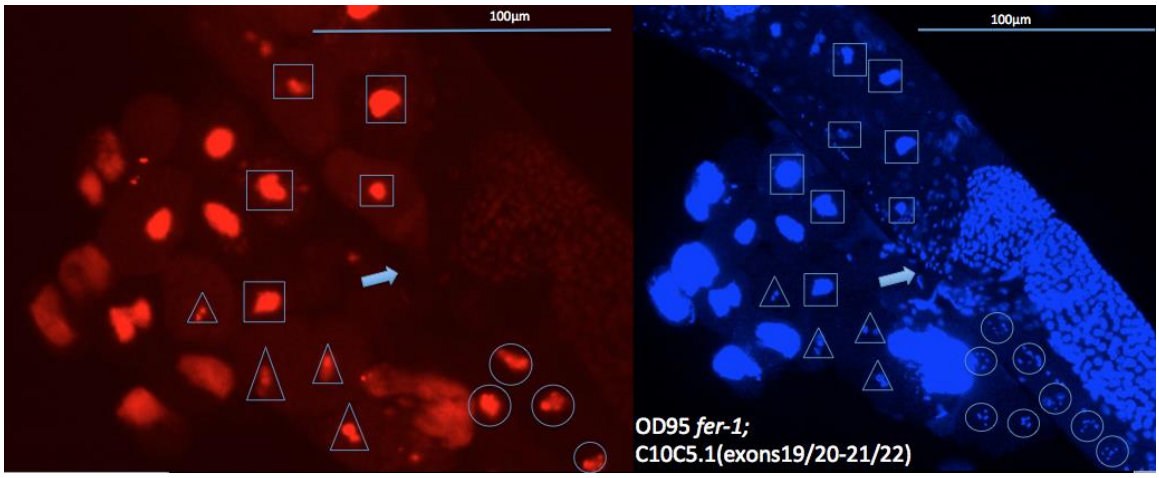

Figure 17. RNAi bacterial feeding with C10C5.1 (exons19/20-21/22) in OD95 *fer-1(b232ts)*I; *ltIs37*IV*; ltIs38* strain. One worm showed penetrance RNAi feeding on one arm with extruded oocytes and staining revealed nonEmo oocytes extruded in close proximity to the vulva (arrow). Laid, nonEmo oocytes (circled) are close to the body while laid Emo oocytes (boxes) are farther away from the worm body, suggesting that nonEmo oocytes will turn Emo at some point after they are laid (triangles) due to an unknown mechanism. Above is the worm shown with mCherry (left) and with DAPI staining (right). 20x, 25°C. n=24.

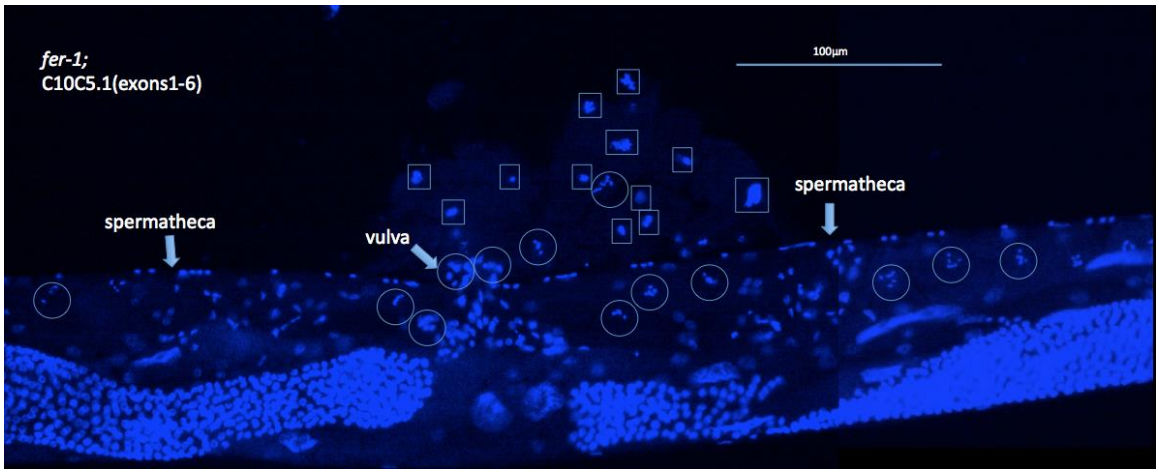

Figure 18. RNAi bacterial feeding with C10C5.1 (exons1-6) in the *fer-1* strain. Four worms showed complete penetrance of RNAi feeding in both gonads of the worm. Four worms showed only one gonad affected. Here you can see that on both sides of the vulva inside of the worm and just extruded oocytes are nonEmo (circled). The oocytes that are laid and farthest away from the vulva are Emo (boxed). Nuclei stained with DAPI; 20x, 25°C. n=16.

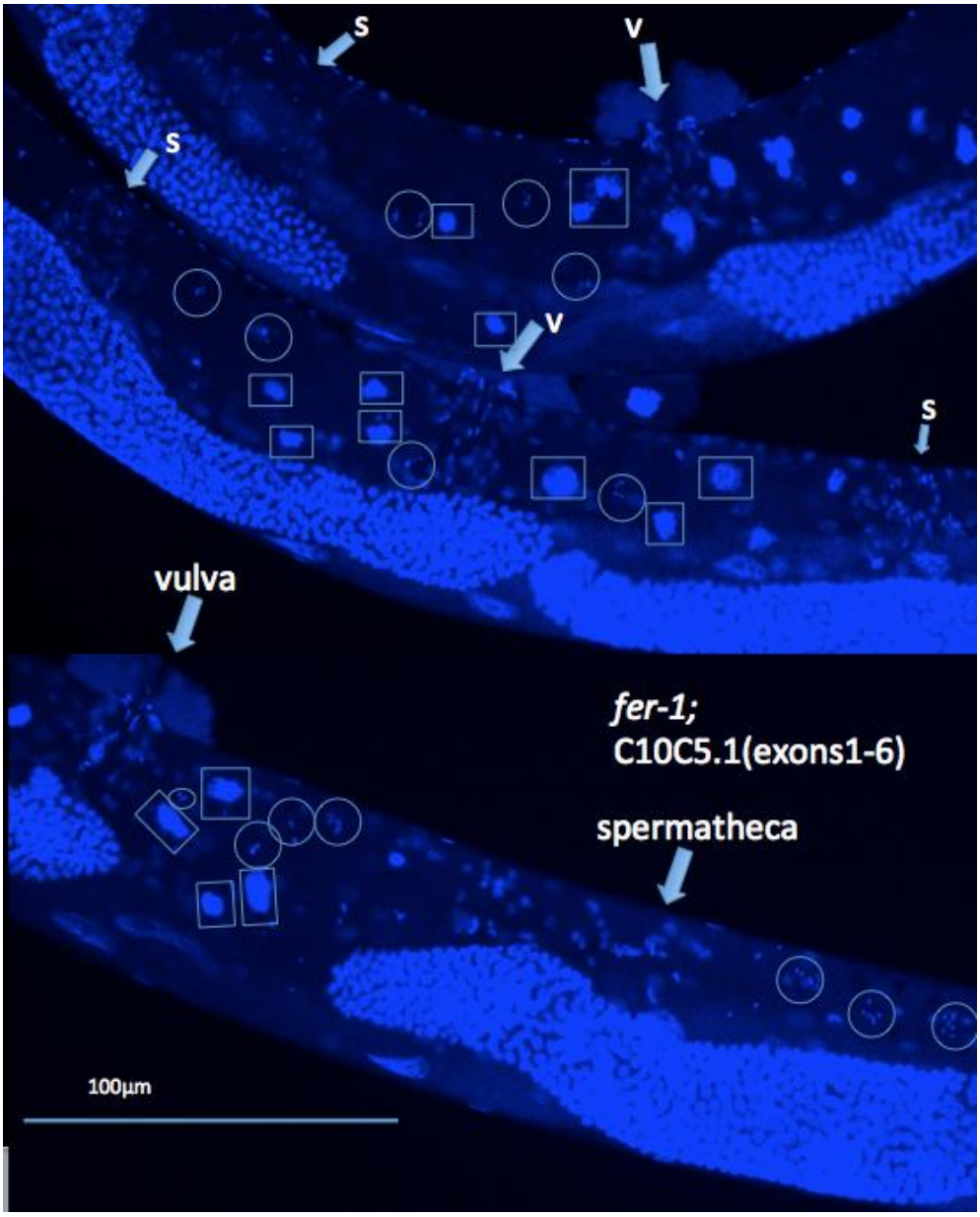

Figure 19. RNAi bacterial feeding with C10C5.1 (exons1-6) in the *fer-1* strain. In addition to showing gonad arm specific differences within the same worm, in three cases, a mixture of both nonEmo and Emo oocytes is evident in the same gonad. NonEmo oocytes (circled) are shown in between oocytes that have already turned Emo (in rectangles). Nuclei stained with DAPI; 20x, 25°C. n=16.

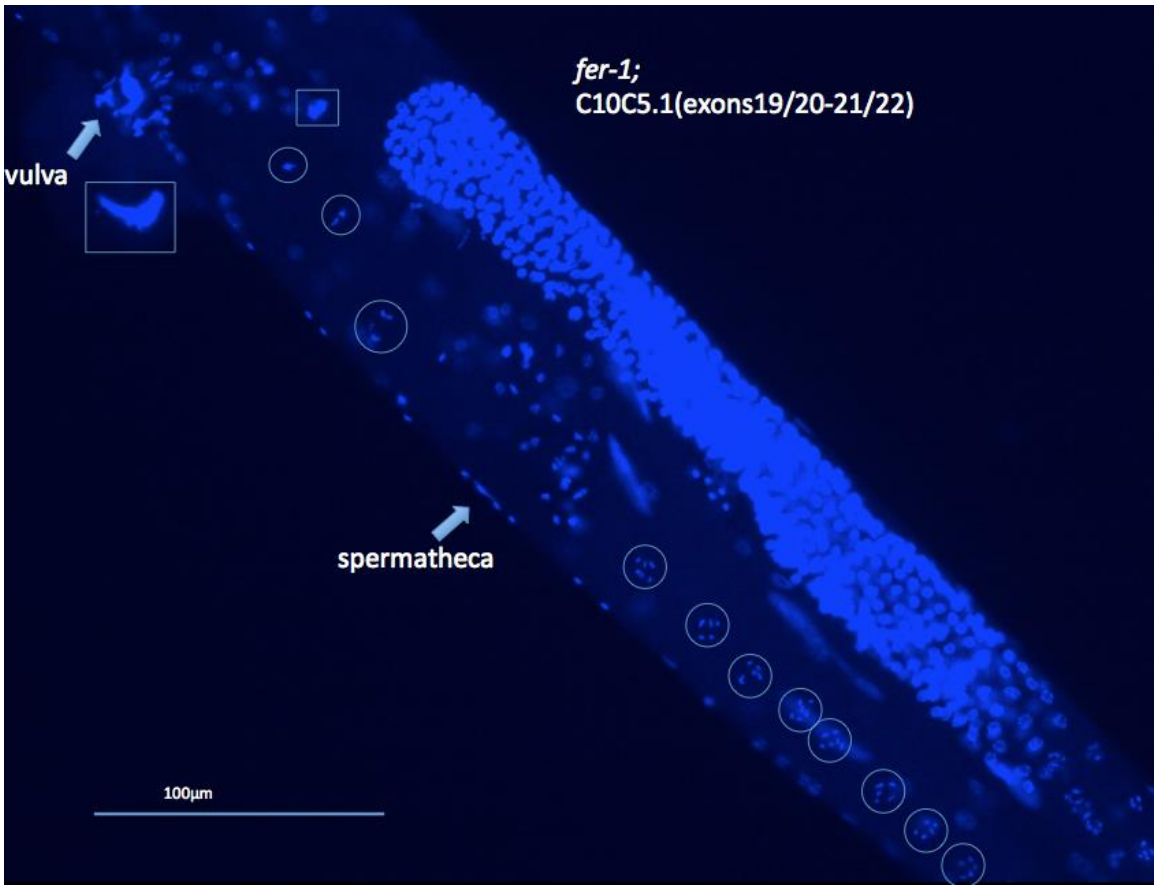

Figure 20. RNAi bacterial feeding with C10C5.1 (exons19/20-21/22) in the *fer-1* strain. Four worms showed one gonad that had oocytes with the nonEmo phenotype. Nuclei stained with DAPI; 20x, 25°C. n=5

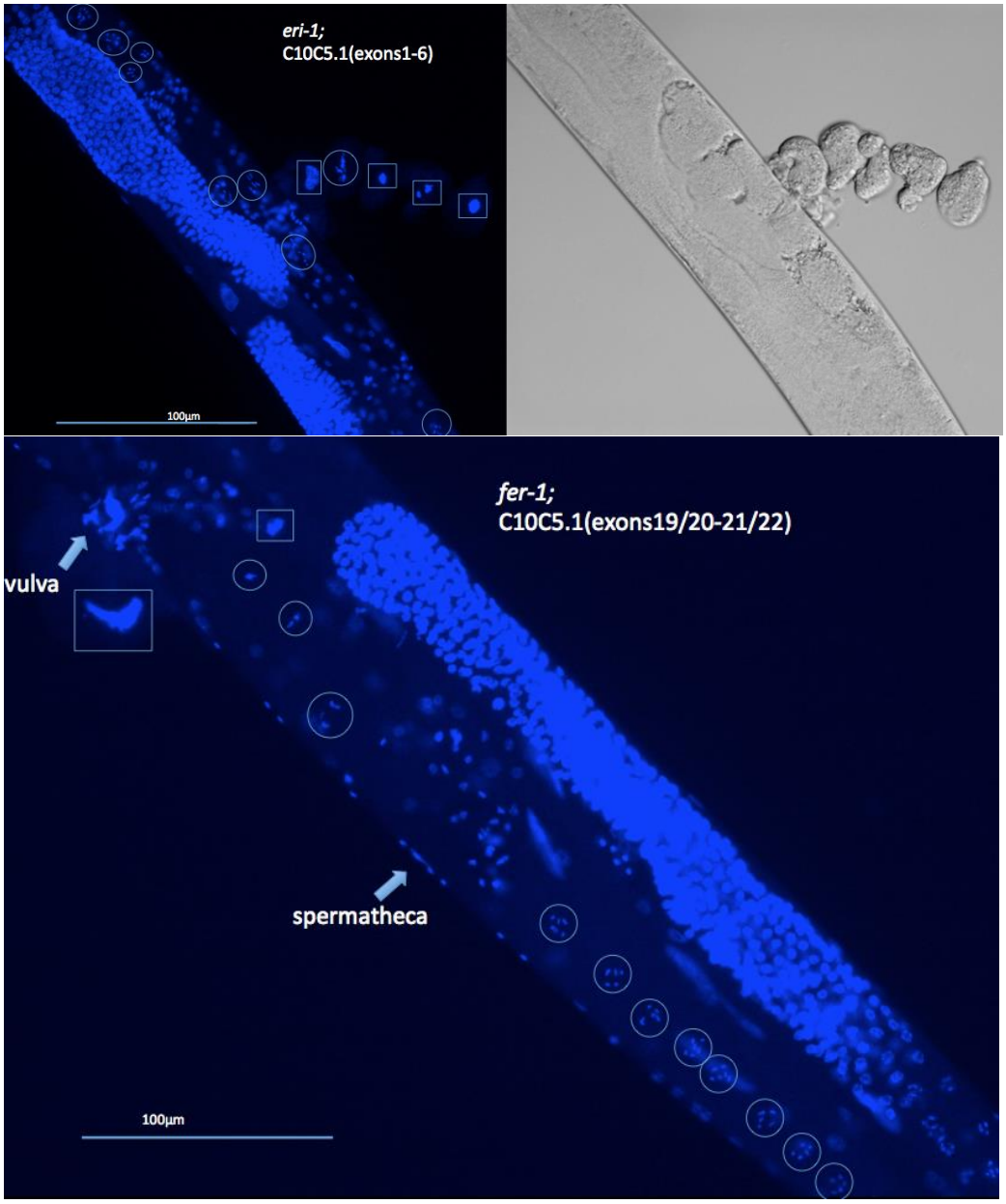

Figure 21. RNAi bacterial feeding with C10C5.1 (exons1-6) in the *eri-1* strain. Four worms showed nonEmo oocytes in both gonads. Six worms showed nonEmo oocytes in only one gonad arm. Above you can see RNAi penetrance in both gonad arms with nonEmo oocytes on either side of the vulva (circled) and with a nonEmo oocyte extruded amongst other Emo oocytes (squared). Nuclei stained with DAPI with DIC correlate; 20x, 25°C. n=21.

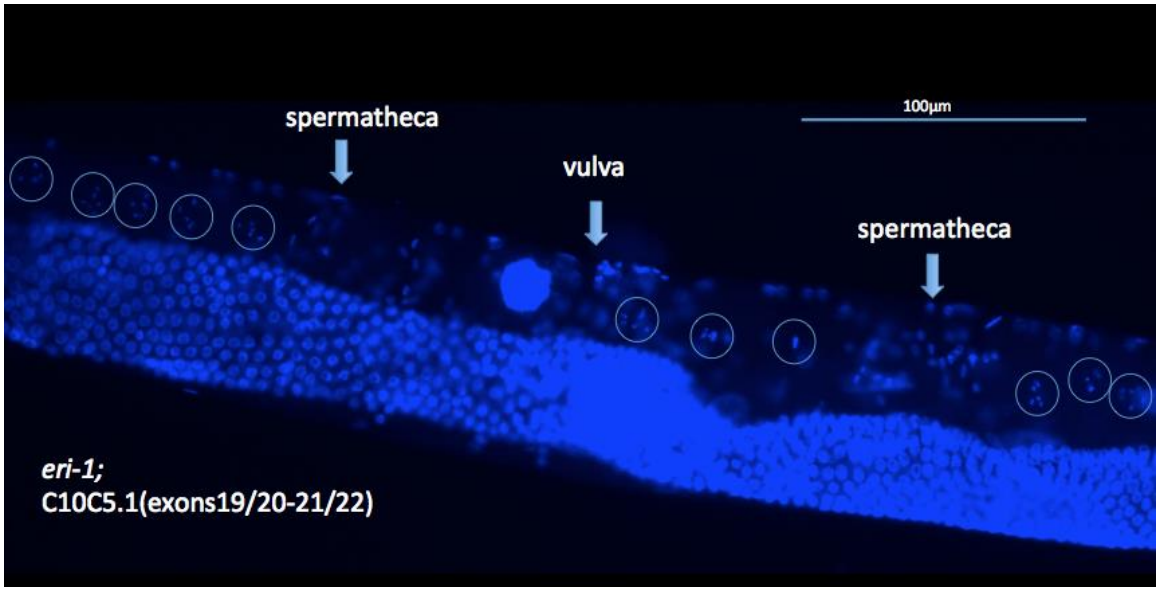

Figure 22. RNAi bacterial feeding with C10C5.1 (exons19/20-21/22) in the *eri-1* strain. One worm showed to have nonEmo oocytes past the spermatheca towards the vulva (circled) in both gonads. Nuclei stained with DAPI; 20x, 25°C. n=4.

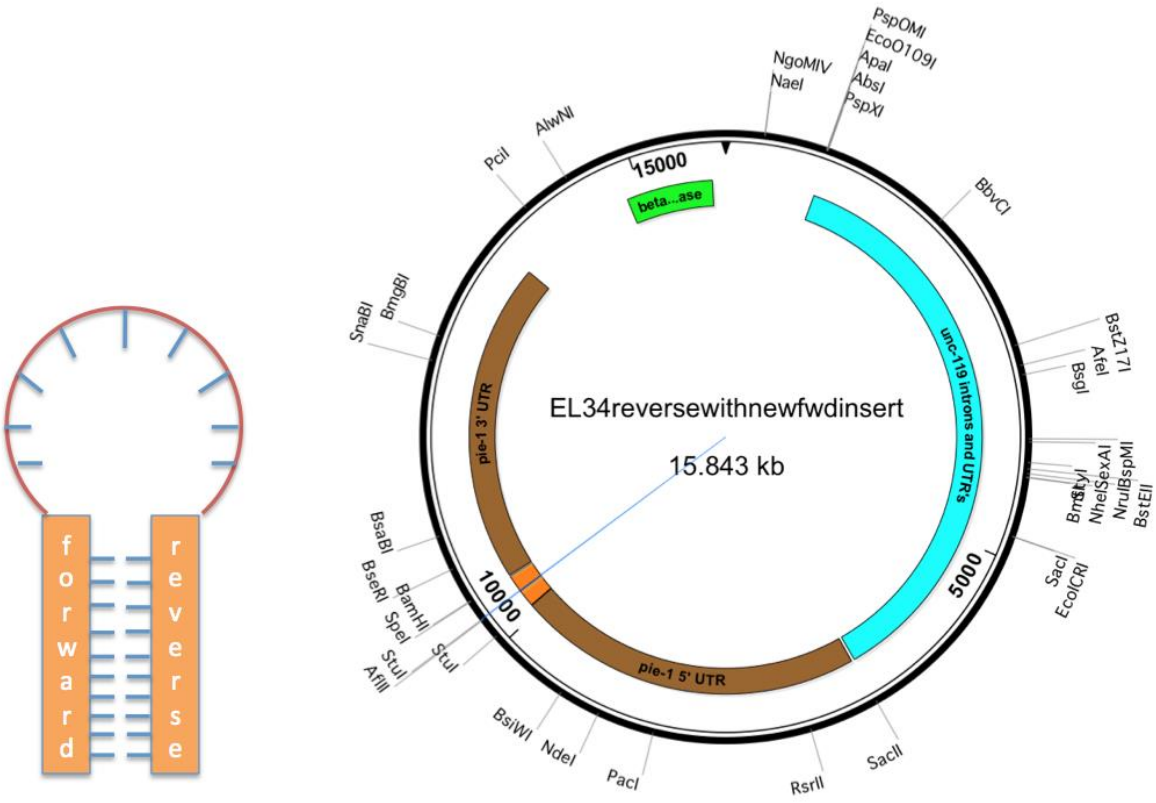

Figure 23. Shows the design of the RNAi hairpin plasmid using pHF10 background and *pezo-1* inserts in the forward and reverse directions.

References

1. Brenner, S. (1974). The genetics of *Caenorhabditis elegans*. Genetics *77*, 71-94.
2. Madl, J.E., and Herman, R.K. (1979). Polyploids and sex determination in *Caenorhabditis elegans*. Genetics *93*, 393-402.
3. Emmons, S.W. (2014). The development of sexual dimorphism: studies of the *Caenorhabditis elegans* male. Wiley Interdiscip Rev Dev Biol *3*, 239-262.
4. Akerib, C.C., and Meyer, B.J. (1994). Identification of X-chromosome regions in *Caenorhabditis elegans* that contain sex-determination signal elements. Genetics *138*, 1105-1125.
5. Kimble, J., and Hirsh, D. (1979). The postembryonic cell lineages of the hermaphrodite and male gonads in *Caenorhabditis elegans*. Dev Bio *70*, 396-417.
6. Herman, M.A. (2006). Hermaphrodite cell-fate specification. WormBook : the online review of *C. elegans* biology, 1-16.
7. Hodgkin, J., Horvitz, H.R., and Brenner, S. (1979). Nondisjunction mutants of the nematode *Caenorhabditis elegans*. Genetics *91*, 67-94.
8. Klass, M., Wolf, N., and Hirsh, D. (1976). Development of the male reproductive system and sexual transformation in the nematode *Caenorhabditis elegans.* Dev Bio *52*, 1-18.
9. Hirsh, D., Oppenheim, D., and Klass, M. (1976). Development of the reproductive system of *Caenorhabditis elegans*. Dev Bio *49*, 200-219.
10. Kimble, J.E., and White, J.G. (1981). On the control of germ cell development in *Caenorhabditis elegans*. Dev Bio *81*, 208-219.
11. Byrd, D.T., Knobel, K., Affeldt, K., Crittenden, S.L., and Kimble, J. (2014). A DTC niche plexus surrounds the germline stem cell pool in *Caenorhabditis elegans.* PloS one *9*, e88372.
12. Crittenden, S.L., Leonhard, K.A., Byrd, D.T., and Kimble, J. (2006). Cellular analyses of the mitotic region in the *Caenorhabditis elegans* adult germ line. Mol Biol Cell *17*, 3051-3061.
13. L'Hernault, S.W. (2009). The genetics and cell biology of spermatogenesis in the nematode *C. elegans*. Mol Cell Endocrin *306*, 59-65.
14. Ward, S., and Carrel, J.S. (1979). Fertilization and sperm competition in the nematode *Caenorhabditis elegans*. Dev Bio *73*, 304-321.
15. McCarter, J., Bartlett, B., Dang, T., and Schedl, T. (1999). On the control of oocyte meiotic maturation and ovulation in *Caenorhabditis elegans*. Dev Bio *205*, 111-128.
16. L'Hernault, S.W. (2006). Spermatogenesis. WormBook: the online review of *C. elegans* biology, 1-14
17. McCarter, J., Bartlett, B., Dang, T., and Schedl, T. (1997). Soma-germ cell interactions in *Caenorhabditis elegans*: multiple events of hermaphrodite germline development require the somatic sheath and spermathecal lineages. Dev Bio *181*, 121-143.
18. Ellis, R.E., and Kimble, J. (1994). Control of germ cell differentiation in *Caenorhabditis elegans*. Ciba Found Symp *182*, 179-188; discussion 189-192.
19. Ward, S., and Carrel, J.S. (1979). Fertilization and sperm competition in the nematode *Caenorhabditis elegans*. Dev Bio *73*, 304-321.

20. Wolf, N., Hirsh, D., and McIntosh, J.R. (1978). Spermatogenesis in males of the free-living nematode, *Caenorhabditis elegans*. J Ultrastruct Res *63*, 155-169.
21. LaMunyon, C.W., and Ward, S. (1998). Larger sperm outcompete smaller sperm in the nematode *Caenorhabditis elegans*. Proc Biol Sci *265*, 1997-2002.
22. LaMunyon, C.W., and Ward, S. (1995). Sperm precedence in a hermaphroditic nematode (*Caenorhabditis elegans*) is due to competitive superiority of male sperm. Experientia *51*, 817-823.
23. L'Hernault, S.W. (1997). Spermatogenesis. In *C. elegans* II, 2nd Edition, D.L. Riddle, T. Blumenthal, B.J. Meyer and J.R. Priess, eds. (Cold Spring Harbor (NY)).
24. Nishimura, H., and L'Hernault, S.W. (2010). Spermatogenesis-defective (spe) mutants of the nematode *Caenorhabditis elegans* provide clues to solve the puzzle of male germline functions during reproduction. Dev Dyn *239*, 1502-1514.
25. Ward, S., Argon, Y., and Nelson, G.A. (1981). Sperm morphogenesis in wild-type and fertilization-defective mutants of *Caenorhabditis elegans*. J Cell Biol *91*, 26-44.
26. Hirsh, D., and Vanderslice, R. (1976). Temperature-Sensitive Developmental Mutants of *Caenorhabditis elegans*. Dev Bio *49*, 220-235.
27. Singson, A. (2001). Every sperm is sacred: Fertilization in *Caenorhabditis elegans*. Dev Bio *230*, 101-109.
28. L'Hernault, S.W., Shakes, D.C., and Ward, S. (1988). Developmental genetics of chromosome I spermatogenesis-defective mutants in the nematode *Caenorhabditis elegans*. Genetics *120*, 435-452.
29. Klass, M.R., and Hirsh, D. (1981). Sperm isolation and biochemical analysis of the major sperm protein from *Caenorhabditis elegans*. Dev Bio *84*, 299-312.
30. Machaca, K., DeFelice, L.J., and L'Hernault, S.W. (1996). A novel chloride channel localizes to *Caenorhabditis elegans* spermatids and chloride channel blockers induce spermatid differentiation. Dev Bio *176*, 1-16.
31. Nelson, G.A., and Ward, S. (1980). Vesicle fusion, pseudopod extension and amoeboid motility are induced in nematode spermatids by the ionophore monensin. Cell *19*, 457-464.
32. Bae, Y.K., Kim, E., L'Hernault S, W., and Barr, M.M. (2009). The CIL-1 PI 5-phosphatase localizes TRP Polycystins to cilia and activates sperm in *C. elegans*. Current biology : CB *19*, 1599-1607.
33. Ward, S., Hogan, E., and Nelson, G.A. (1983). The initiation of spermiogenesis in the nematode *Caenorhabditis elegans*. Dev Bio *98*, 70-79.
34. LaMunyon, C.W., and Ward, S. (1994). Assessing the viability of mutant and manipulated sperm by artificial insemination of *Caenorhabditis elegans*. Genetics *138*, 689-692.
35. Singson, A., Mercer, K.B., and L'Hernault, S.W. (1998). The *C. elegans spe-9* gene encodes a sperm transmembrane protein that contains EGF-like repeats and is required for fertilization. Cell *93*, 71-79.
36. Gilbert, S.F. (2000). Oogenesis. In *Developmental Biology*. (Sunderland, MA: Sinauer Associates).

37. Ezzati, M., Djahanbakhch, O., Arian, S., and Carr, B.R. (2014). Tubal transport of gametes and embryos: a review of physiology and pathophysiology. J Assist Reprod Genet *31*, 1337-1347.
38. Storey, B.T. (1995). Interactions between gametes leading to fertilization: the sperm's eye view. Reprod Fertil Dev *7*, 927-942.
39. Heffner, L.J., and Schust, D.J. (2014). The reproductive system at a glance, Fourth edition. Edition, (Chichester, West Sussex: John Wiley & Sons, Inc.).
40. Iwasaki, K., McCarter, J., Francis, R., and Schedl, T. (1996). emo-1, a *Caenorhabditis elegans* Sec61p gamma homologue, is required for oocyte development and ovulation. J Cell Biol *134*, 699-714.
41. Phillips, C.M., Wong, C., Bhalla, N., Carlton, P.M., Weiser, P., Meneely, P.M., and Dernburg, A.F. (2005). HIM-8 binds to the X chromosome pairing center and mediates chromosome-specific meiotic synapsis. Cell *123*, 1051-1063.
42. Barnes, T.M., Jin, Y., Horvitz, H.R., Ruvkun, G., and Hekimi, S. (1996). The *Caenorhabditis elegans* behavioral gene *unc-24* encodes a novel bipartite protein similar to both erythrocyte band 7.2 (stomatin) and nonspecific lipid transfer protein. J Neurochem *67*, 46-57.
43. Pohl, K.A. (2015). The Identification and Mapping of a Gene Responsible for a Novel nonEmo Phenotype in *C. elegans* Oocytes. In Biology. (Emory University), 97 pp.
44. Thompson, O., Edgley, M., Strasbourger, P., Flibotte, S., Ewing, B., Adair, R., Au, V., Chaudhry, I., Fernando, L., Hutter, H., et al. (2013). The million mutation project: a new approach to genetics in *Caenorhabditis elegans*. Genome Res *23*, 1749-1762.
45. Zanetti, S., and Puoti, A. (2013). Sex determination in the *Caenorhabditis elegans* germline. Adv Exp Med Biol *757*, 41-69.
46. Maruyama, K., and Sugano, S. (1994). Oligo-capping: a simple method to replace the cap structure of eukaryotic mRNAs with oligoribonucleotides. Gene *138*, 171-174.
47. Schaefer, B.C. (1995). Revolutions in rapid amplification of cDNA ends: new strategies for polymerase chain reaction cloning of full-length cDNA ends. Anal Biochem *227*, 255-273.
48. Xiao, R., and Xu, X.Z.S. (2010). Mechanosensitive Channels: In Touch with Piezo. Curr Biol *20*, R936-R938.
49. Coste, B., Mathur, J., Schmidt, M., Earley, T.J., Ranade, S., Petrus, M.J., Dubin, A.E., and Patapoutian, A. (2010). Piezo1 and Piezo2 are essential components of distinct mechanically activated cation channels. Science *330*, 55-60.
50. Delmas, P., and Coste, B. (2013). Mechano-gated ion channels in sensory systems. Cell *155*, 278-284.
51. Kung, C. (2005). A possible unifying principle for mechanosensation. Nature *436*, 647-654.
52. Martinac, B. (2007). 3.5 billion years of mechanosensory transduction: Structure and function of mechanosensitive channels in prokaryotes. Curr Top Membr *58*, 25-57.

53. Chelur, D.S., Ernstrom, G.G., Goodman, M.B., Yao, C.A., Chen, L., O'Hagan, R., and Chalfie, M. (2002). The mechanosensory protein MEC-6 is a subunit of the *C. elegans* touch-cell degenerin channel. Nature *420*, 669-673.
54. Kang, L., Gao, J., Schafer, W.R., Xie, Z., and Xu, X.Z.S. (2010). *C. elegans* TRP Family Protein TRP-4 Is a Pore-Forming Subunit of a Native Mechanotransduction Channel. Neuron *67*, 381-391.
55. Schafer, W.R. (2015). Mechanosensory molecules and circuits in *C. elegans*. Pflug Arch Eur J Phy *467*, 39-48.
56. Coste, B., Xiao, B.L., Santos, J.S., Syeda, R., Grandl, J., Spencer, K.S., Kim, S.E., Schmidt, M., Mathur, J., Dubin, A.E., et al. (2012). Piezo proteins are pore-forming subunits of mechanically activated channels. Nature *483*, 176-U172.
57. Ge, J.P., Li, W.Q., Zhao, Q.C., Li, N.N., Chen, M.F., Zhi, P., Li, R.C., Gao, N., Xiao, B.L., and Yang, M.J. (2015). Architecture of the mammalian mechanosensitive Piezol channel. Nature *527*, 64-69.
58. Albuisson, J., Murthy, S.E., Bandell, M., Coste, B., Louis-dit-Picard, H., Mathur, J., Feneant-Thibault, M., Tertian, G., de Jaureguiberry, J.P., Syfuss, P.Y., et al. (2013). Dehydrated hereditary stomatocytosis linked to gain-of-function mutations in mechanically activated PIEZO1 ion channels. Nat Commun *4*, 1884, 2013
59. Fotiou, E., Martin-Almedina, S., Simpson, M.A., Lin, S., Gordon, K., Brice, G., Atton, G., Jeffery, I., Rees, D.C., Mignot, C., et al. (2015). Novel mutations in PIEZO1 cause an autosomal recessive generalized lymphatic dysplasia with non-immune hydrops fetalis. Nat Commun *6*, 8085.
60. Bae, C., Gnanasambandam, R., Nicolai, C., Sachs, F., and Gottlieb, P.A. (2013). Xerocytosis is caused by mutations that alter the kinetics of the mechanosensitive channel PIEZO1. Proc Natl Acad Sci (USA) *110*, E1162-1168.
61. Gottlieb, P.A., Bae, C., and Sachs, F. (2012). Gating the mechanical channel Piezo1 A comparison between whole-cell and patch recording. Channels *6*, 282-289.
62. Akyuz, N., and Holt, J.R. (2016). Plug-N-Play: Mechanotransduction Goes Modular. Neuron *89*, 1128-1130.
63. Silberberg, S.D., and Magleby, K.L. (1997). Voltage-induced slow activation and deactivation of mechanosensitive channels in *Xenopus* oocytes. J Physiol *505 (Pt 3)*, 551-569.
64. Hamill, O.P., and McBride, D.W., Jr. (1997). Mechanogated channels in *Xenopus* oocytes: different gating modes enable a channel to switch from a phasic to a tonic mechanotransducer. Biol Bull *192*, 121-122.
65. Huang, H., Kamm, R.D., and Lee, R.T. (2004). Cell mechanics and mechanotransduction: pathways, probes, and physiology. Am J Physiol Cell Physiol *287*, C1-11.
66. Jahed, Z., Shams, H., Mehrbod, M., and Mofrad, M.R. (2014). Mechanotransduction pathways linking the extracellular matrix to the nucleus. Int Rev Cell Mol Biol *310*, 171-220.
67. Miller, M.A., Nguyen, V.Q., Lee, M.H., Kosinski, M., Schedl, T., Caprioli, R.M., and Greenstein, D. (2001). A sperm cytoskeletal protein that signals oocyte meiotic maturation and ovulation. Science *291*, 2144-2147.

68. Pulak, R., and Anderson, P. (1993). mRNA surveillance by the *Caenorhabditis elegans smg* genes. Genes Dev *7*, 1885-1897.
69. Blumenthal, T., and Gleason, K.S. (2003). *Caenorhabditis elegans* operons: form and function. Nat Rev Genet *4*, 112-120.
70. Green, R.A., Kao, H.L., Audhya, A., Arur, S., Mayers, J.R., Fridolfsson, H.N., Schulman, M., Schloissnig, S., Niessen, S., Laband, K., et al. (2011). A high-resolution C. elegans essential gene network based on phenotypic profiling of a complex tissue. Cell *145*, 470-482.
71. Ohkumo, T., Masutani, C., Eki, T., and Hanaoka, F. (2008). Use of RNAi in *C. elegans*. Meth Mol Biol *442*, 129-137.
72. Ahringer, J. (2006). Reverse Genetics. WormBook : the online review of *C. elegans* biology.
73. Fire, A., Xu, S., Montgomery, M.K., Kostas, S.A., Driver, S.E., and Mello, C.C. (1998). Potent and specific genetic interference by double-stranded RNA in *Caenorhabditis elegans*. Nature *391*, 806-811.
74. Grishok, A. (2005). RNAi mechanisms in *Caenorhabditis elegans*. FEBS Letters *579*, 5932-5939.
75. Shih, J.D., and Hunter, C.P. (2011). SID-1 is a dsRNA-selective dsRNA-gated channel. RNA (New York, N.Y.) *17*, 1057-1065.
76. Simmer, F., Tijsterman, M., Parrish, S., Koushika, S.P., Nonet, M.L., Fire, A., Ahringer, J., and Plasterk, R.H. (2002). Loss of the putative RNA-directed RNA polymerase RRF-3 makes *C. elegans* hypersensitive to RNAi. Curr Biol *12*, 1317-1319.
77. Simmer, F., Moorman, C., van der Linden, A.M., Kuijk, E., van den Berghe, P.V., Kamath, R.S., Fraser, A.G., Ahringer, J., and Plasterk, R.H. (2003). Genome-wide RNAi of *C. elegans* using the hypersensitive *rrf-3* strain reveals novel gene functions. PLoS Biol *1*, E12.
78. Gabel, H.W., and Ruvkun, G. (2008). The exonuclease ERI-1 has a conserved dual role in 5.8S rRNA processing and RNAi. Nat Struct Mol Biol *15*, 531-533.
79. Zhuang, J.J., and Hunter, C.P. (2011). Tissue specificity of *Caenorhabditis elegans* enhanced RNA interference mutants. Genetics *188*, 235-237.
80. Zhuang, J.J., and Hunter, C.P. (2012). RNA interference in *Caenorhabditis elegans*: uptake, mechanism, and regulation. Parasitology *139*, 560-573.
81. Fraser, A.G., Kamath, R.S., Zipperlen, P., Martinez-Campos, M., Sohrmann, M., and Ahringer, J. (2000). Functional genomic analysis of *C. elegans* chromosome I by systematic RNA interference. Nature *408*, 325-330.
82. Kamath, R.S., Fraser, A.G., Dong, Y., Poulin, G., Durbin, R., Gotta, M., Kanapin, A., Le Bot, N., Moreno, S., Sohrmann, M., et al. (2003). Systematic functional analysis of the *Caenorhabditis elegans* genome using RNAi. Nature *421*, 231-237.
83. Blelloch, R., Anna-Arriola, S.S., Gao, D., Li, Y., Hodgkin, J., and Kimble, J. (1999). The gon-1 gene is required for gonadal morphogenesis in *Caenorhabditis elegans*. Dev Bio *216*, 382-393.
84. Merritt, C., and Seydoux, G. (2010). Transgenic solutions for the germline. WormBook : the online review of *C. elegans* biology, 1-21.

85. Kelly, W.G., Xu, S., Montgomery, M.K., and Fire, A. (1997). Distinct requirements for somatic and germline expression of a generally expressed *Caernorhabditis elegans* gene. Genetics *146*, 227-238.
86. Mello, C.C., Schubert, C., Draper, B., Zhang, W., Lobel, R., and Priess, J.R. (1996). The PIE-1 protein and germline specification in *C. elegans* embryos. Nature *382*, 710-712.
87. Merritt, C., Rasoloson, D., Ko, D., and Seydoux, G. (2008). 3' UTRs are the primary regulators of gene expression in the *C. elegans* germline. Curr Biol *18*, 1476-1482.
88. Moore, C.B., Guthrie, E.H., Huang, M.T., and Taxman, D.J. (2010). Short hairpin RNA (shRNA): design, delivery, and assessment of gene knockdown. Methods Mol Biol *629*, 141-158.
89. Raleigh, E.A., and Wilson, G. (1986). Escherichia coli K-12 restricts DNA containing 5-methylcytosine. Proc Natl Acad Sci (USA) *83*, 9070-9074.
90. Kelleher, J.E., and Raleigh, E.A. (1991). A novel activity in *Escherichia coli* K-12 that directs restriction of DNA modified at CG dinucleotides. J Bacteriol *173*, 5220-5223.
91. Weiserova, M., and Ryu, J. (2008). Characterization of a restriction modification system from the commensal *Escherichia coli* strain A0 34/86 (O83:K24:H31). BMC Microbiol *8*, 106.
92. Gleason, E.J., Lindsey, W.C., Kroft, T.L., Singson, A.W., and L'Hernault S, W. (2006). *spe-10* encodes a DHHC-CRD zinc-finger membrane protein required for endoplasmic reticulum/Golgi membrane morphogenesis during *Caenorhabditis elegans* spermatogenesis. Genetics *172*, 145-158.
93. Calixto, A., Chelur, D., Topalidou, I., Chen, X., and Chalfie, M. (2010). Enhanced neuronal RNAi in *C. elegans* using SID-1. Nat Meth *7*, 554-559.
94. Updike, D.L., and Strome, S. (2009). A genomewide RNAi screen for genes that affect the stability, distribution and function of P granules in *Caenorhabditis elegans*. Genetics *183*, 1397-1419.
95. Samuelson, A.V., Klimczak, R.R., Thompson, D.B., Carr, C.E., and Ruvkun, G. (2007). Identification of *Caenorhabditis elegans* genes regulating longevity using enhanced RNAi-sensitive strains. Cold Sp Hbr Symp Quant Biol *72*, 489-497.
96. Kobayashi, I., Tsukioka, H., Komoto, N., Uchino, K., Sezutsu, H., Tamura, T., Kusakabe, T., and Tomita, S. (2012). SID-1 protein of *Caenorhabditis elegans* mediates uptake of dsRNA into Bombyx cells. Insect Biochem Mol Biol *42*, 148-154.
97. Boutros, M., and Ahringer, J. (2008). The art and design of genetic screens: RNA interference. Nat Rev Genet *9*, 554-566.
98. Reinke, V., and Cutter, A.D. (2009). Germline expression influences operon organization in the *Caenorhabditis elegans* genome. Genetics *181*, 1219-1228.
99. Blumenthal, T., Evans, D., Link, C.D., Guffanti, A., Lawson, D., Thierry-Mieg, J., Thierry-Mieg, D., Chiu, W.L., Duke, K., Kiraly, M., et al. (2002). A global analysis of *Caenorhabditis elegans* operons. Nature *417*, 851-854.
100. Kumsta, C., and Hansen, M. (2012). *C. elegans rrf-1* mutations maintain RNAi efficiency in the soma in addition to the germline. PloS One *7*, e35428.

101. Crittenden, S.L., Troemel, E.R., Evans, T.C., and Kimble, J. (1994). GLP-1 is localized to the mitotic region of the *C. elegans* germ line. Development *120*, 2901-2911.
102. Hubbard, E.J., and Greenstein, D. (2005). Introduction to the germ line. WormBook : the online review of *C. elegans* biology, 1-4.
103. Austin, J., and Kimble, J. (1987). *glp-1* is required in the germ line for regulation of the decision between mitosis and meiosis in *C. elegans*. Cell *51*, 589-599.
104. Han, S.M., Cottee, P.A., and Miller, M.A. (2010). Sperm and oocyte communication mechanisms controlling *C. elegans* fertility. Dev Dyn *239*, 1265-1281.
105. Grant, B., and Hirsh, D. (1999). Receptor-mediated endocytosis in the *Caenorhabditis elegans* oocyte. Mol Biol Cell *10*, 4311-4326.